TECHNISCHE
UNIVERSITÄT
WIEN
Vienna University of Technology

Master Thesis

ASYMMETRIC SYNTHESIS OF WARFARIN DERIVATES *VIA* HOMOGENOUS AND HETEROGENOUS IMINIUM CATALYSIS

Ausgeführt am
Institut für Angewandte Synthesechemie

unter der Leitung von
Univ. Prof. Dipl.-Ing. Dr. techn. Katharina Schröder
und
Assoc. Prof. Dipl.-Ing. Dr. techn. Michael Schnürch

eingereicht an der Technischen Universität Wien
am
von

Ismael Salhi BSc.
[redacted]

Table of Contents

Danksagung

Zuallererst möchte ich mich bei allen Personen bedanken, die mir die Möglichkeit gaben, meine Diplomarbeit zu machen und mich dabei begleiteten und unterstützten. Ganz Besonders geht mein Dank an Univ.-Prof. Katharina Schröder und Assoc. Prof. Dipl.-Ing. Dr. techn. Michael Schnürch, die mir die Diplomarbeit ermöglicht und die Chance gaben, meine Fähigkeiten als angehender Wissenschaftler zu erweitern. Sie gaben mir nicht nur die Möglichkeit, sondern halfen mir auch sehr während der Diplomarbeit. Ich möchte mich auch bei meinem Co-Betreuer Dipl.-Ing. Fabian Scharinger herzlichst für die Unterstützung und die zahlreichen Tipps, sowie den zahlreichen Gesprächen- bedanken, die mir bei diesem Projekt weiterhalfen. Mein Dank gebührt auch der ganzen Forschungsgruppe von Frau Professor Schröder, die mir auch während der Diplomarbeit, durch ihre Tipps und Tricks, sowie das angenehme Arbeitsklima, die Zeit zu einem schönen Erlebnis machten. In diesem Sinne geht ein besonderer Dank an Ádám Márk Pálvölgyi, Olga Lanaridi, Aitor Sainz Martinez, Philipp Miksovsky, Kristof Stagel, Lisa Eisele, Julia Agnieszka Piotrowska und Jasmina Vukovič. Ein außerordentlicher Dank geht auch an meine Eltern und meiner Schwester, die mich motivierten und bestärkten.

Abstract

This work is dedicated to the synthesis of warfarin and its analogues *via* acid-assisted asymmetric iminium catalysis, as well as the immobilisation of the catalyst and set-up of the reactions in continuous mode. This novel approach involves an amino acid-derived diamine catalyst, which comprises a primary and tertiary amine moiety in combination with different atropisomeric flexible phosphoric acids or TFA. After proving the concept of diamine-catalysis, several parameters including the solvent, catalyst components and reaction conditions were screened to identify optimum conditions. Once the ideal diamine and acidic part, as well as the ideal conditions for iminium catalysis of warfarin derivates, were figured out, the pool of starting materials was widened to include various substrates rather than 4-hydroxycoumarin. High yields and enantioselectivities could be achieved with various substrates, thereby proving the versatility of the newly developed concept of the iminium catalyst. To extend the versatility of the amino-acid derived catalyst, the scope was widened to the immobilisation of the catalyst *via* chemisorption and/or physisorption on a silica- or polyoxotungstate-support.

Kurzfassung

Diese Arbeit widmet sich der Synthese von Warfarin-Analoga und auch Warfarin selbst, mittels säureunterstützter asymmetrischer Iminiumkatalyse, sowie der Immobilisierung des Katalysators und folglich der Vorbereitung für flusschemische Experimente. In diesem Konzept werden Diamine, die mit einer primären und tertiären Amineinheit ausgestattet und aus Aminosäuren hergeleitet sind, in Kombination mit verschiedenen atropisomeren flexiblen Phosphorsäuren oder TFA, verwendet. Nachdem das Konzept der Diaminkatalyse nachgewiesen wurde, wurden verschiedene Parameter, wie Lösungsmittel, katalytische Komponenten, sowie die Reaktionsbedingungen, untersucht. Nach Auswahl des katalytischen Systems und den idealen Reaktionsbedingungen, wurden, neben 4-Hydroxycoumarin, weitere Substrate untersucht. Es wurden hohe Enantioselektivitäten und Ausbeuten, für die verschiedenen Substrate erreicht. Um die Vielseitigkeit des katalytischen Systems zu erweitern, wurde dieser, mittels Chemisorption und/oder Physisorption, an Silica oder Polyoxowolframat immobilisiert.

1 Introduction

1.1 Warfarin

Warfarin is one of the most potent anticoagulants on the market and has been licensed since 1954. Usually, it is prescribed as treatment for venous thromboembolism and occasionally for atrial fibrillation and cardiac valve replacement.[1] Warfarin is also known by the trade name Coumadin® on the market.[2] While it is widely used in North America, Southeast Asia, and various other countries, its usage is not as common in Europe. Warfarin is not as readily available in Europe, especially in Austria and Switzerland. Phenprocoumon, or Marcumar, is more frequently used as a substitute.

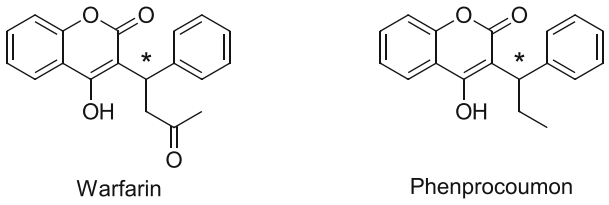

Figure 1: Molecular structures of warfarin (left) and phenprocoumon (right)

The structural difference between warfarin and phenprocoumon is the acetyl moiety at the aliphatic part. Both have the exact mechanism of action and side effects, similar chemical properties and are used as racemates, with the *(S)*-enantiomer being the more potent one. Even though they have many similarities in their chemical nature, they still have some differences. For example, warfarin is mainly metabolised via the enzyme CYP2C9 in the liver, while the enzyme CYP3A4 is responsible for the metabolisation of phenprocoumon.[3,4] As previously stated, both enantiomers of warfarin possess anticoagulant properties, which is a significant advantage. However, the *(S)*-enantiomer is more potent than the *(R)*-enantiomer. Generally, the biological activity of *(S)*-warfarin is 5-8 times higher than the *(R)*-enantiomer.[5] However, warfarin is synthesised and marketed as a racemic mixture, since the enantioselective synthesis of warfarin is challenging and expensive. Warfarin is synthesised from 4-hydroxycoumarin and benzylidene acetone *via* acid/base driven Michael addition (Figure 2).[5]

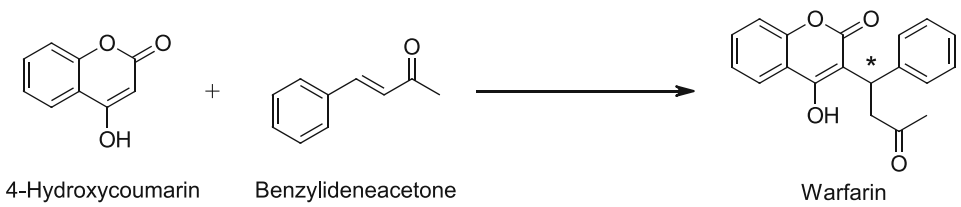

Figure 2: General reaction for the synthesis of warfarin

Different approaches, such as enzymatic[6,7] and organocatalytic[8,9] processes, were studied for its asymmetric synthesis. The first results were reported in 2012 by the group of Bang-Hua Xie et al., who used lipase enzymes obtained from the pancreas of pigs. The results showed poor enantioselectivity with 22% ee at peak, albeit the yield being quite good with a maximum of 84%. Yet the reaction time of 102 hours is a significant disadvantage.[6] Since then, no additional investigations on enzyme-catalysed Michael-Addition on warfarin have been published. The focus has mainly remained on organocatalysts, which are environmentally benign and easy to synthesise. Especially amine-catalysts have proved their potential for the synthesis of warfarin. Different approaches have been developed over time. A quinine-derived primary amine was one of the first catalysts used in the synthesis of warfarin (Figure 3, left). Specifically, the catalyst was the amine analogue of quinine, comprising a primary amine instead of an alcohol group. Quinine is known as an additive in tonic water or for treating malaria. It is easy to synthesise via the catalytic amination of alcohols – a reaction that can be applied for extensive batch synthesis in the industry. Xie et al. reported promising yields of 86% and an enantiomeric excess of 96% for warfarin by emplyong this catalyst.[10] In the last five years, two major investigations on the synthesis of warfarin have been reported. Kucherenko et al. discovered a "green" alternative for the synthesis of warfarin, using quinoline-based 1,2-diamines (Figure 3, middle), obtaining a yield of 82% and 92% ee.[11] Even though there are catalysts that are suitable for the synthesis of warfarin, a catalyst for the Michael-addition of cyclic enones and Michael donors is barely investigated. In another reported approach, C_2-symmetric squaramide-based primary diamines, which included four secondary amines for hydrogen bonding and two primary amines for iminium formation, were used as catalyst (Figure 3, right). With this catalyst, Kochetkov and co-workers were able to achieve yields of 96% for the (*S*)-enantiomer and 94% for the (*R*)-enantiomer, as well as 96% ee for the (*R*)-enantiomer and 94% ee for the (*S*)-enantiomer.[12]

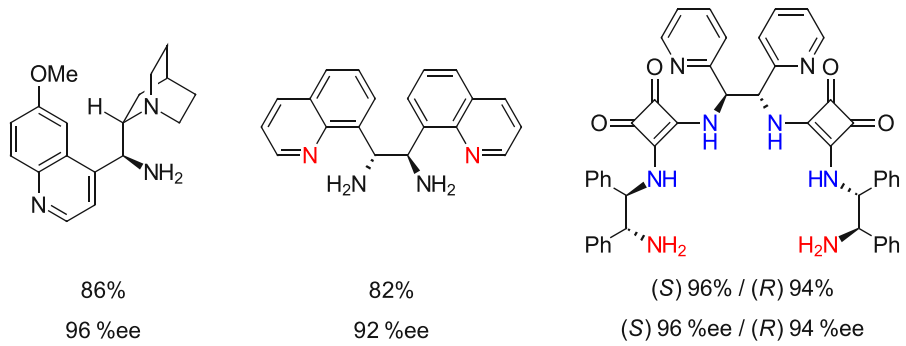

Figure 3: Different organocatalysts for the synthesis of warfarin

1.2 Catalysis

As exemplified above, synthesising (enantiopure) warfarin and its analogues relies heavily on catalytic protocols. Catalysis is indispensable in our everyday lives, whether in industry, pharmacy, research or

even biochemical processes. Since antiquity, catalysts have been essential in fermentation processes in wine and vinegar production, implemented using enzymes. The term "catalyst" is derived from the Greek word "καταλύειν" (katalýein), which means "to annul" or "to untie". Even though catalysts have been used unwittingly since ancient times, the concept of catalysis was primarily invented by the British chemist Elizabeth Fulhame in 1794.[13] In 1811, Gottlieb Kirchhoff succeeded in using a catalyst in organic chemistry for the first time to convert starch to glucose by acid catalysis. Later, the term "catalysis" was cooined by Jöns Jakob Berzelius. A more accurate definition was later presented by Wilhelm Ostwald, as follows:

"A catalyst is a substance that accelerates a reaction, without being consumed nor changing the thermodynamical equilibrium of this reaction."

In general, a catalyst lowers the activation energy (E_a) of the reaction by forming an intermediate with one or both reactants (Figure 4).[14] As a result, less energy is needed to convert the reaction partners to the desired product. However, the standard free enthalpy, also standard Gibbs-energy, ΔG^0, remains identical for a reaction, regardless of the presence or absence of a catalyst. The catalyst cannot shift the equilibrium; in general, the catalyst cannot make a thermodynamically impossible reaction feasible. Catalysts only affect the reaction speed.[15]

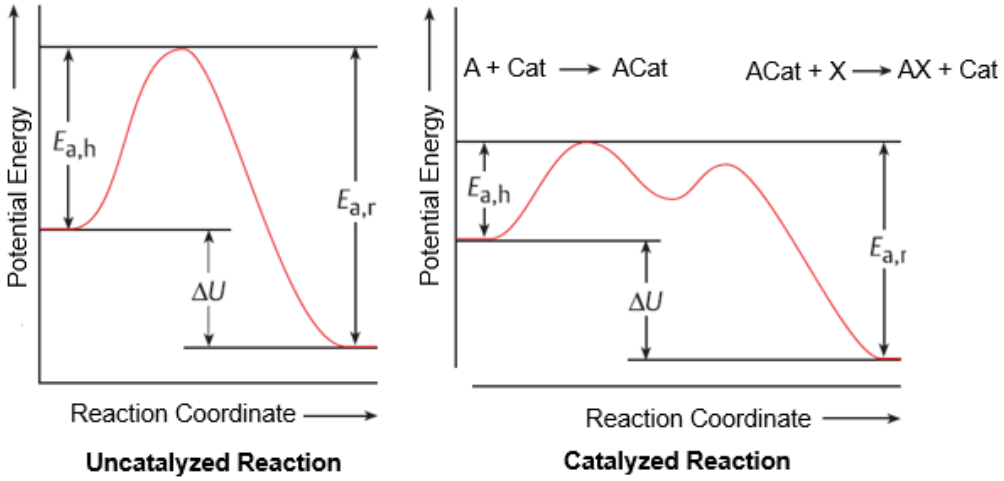

Figure 4: Difference between reaction with and without a catalyst[14]

As previously stated, catalysts can speed up a reaction without being consumed. This means that the catalyst will be reformed after the formation of the product(s). Hence, the catalyst can undergo several "turnovers".[16] This property is beneficial since stoichiometric amounts are not required for a reaction to take place. With a small amount of catalyst, the conversion of a large amount of substance is possible, thus rendering procedures employing catalysts more environmentally friendly and cost-efficient than non-catalysed processes.

1.3 Organocatalysis

Over the last few decades, transition metal complexes and enzymes have primarily dominated the field of catalysis for the enantioselective synthesis of pharmaceuticals, agricultural products, fine chemicals, and synthetic intermediates. While biocatalysts exhibit high selectivity, activity, and stability in the presence of moisture and air, their application range is limited by the narrow substrate scope and specific reaction conditions required. Metal-organic catalysts are adjustable in bulkiness, selectivity, and activity, as well as their high-temperature stability, allowing a much broader application range than biocatalysts. However, most metals, especially rare earth metals, are susceptible to moisture and air.[17] In addition, the future availability of metal elements poses a challenge to the continued use of transition metal complexes as catalysts. For example, rhodium, a crucial catalyst in industry such as automotive manufacturing and the Oswald process, and organic chemistry for reactions such as hydrogenation and hydroboration, is expected to become increasingly scarce and primary sources might eventually run out.[18,19]

In the previous decades, organocatalysis proved its high potential for asymmetric catalysis of various reactions. The typically employed catalysts exhibit robustness and stability towards moisture and air and are commercially available or easy to prepare. Also, they are cheap and non-toxic. However, many organocatalysts require high loadings to provide efficient/satisfactory catalytic activity and, at the same time, they have limited substrate and reaction scope.[17]

In many cases, organocatalysts have mechanisms of action analogous to enzymes. A representative example is the catalysis of aldol reactions, where lysine provides the catalytic active site of the enzyme class-I aldolases. In terms of organocatalysis, enamine formation is the kay intermediate.[20,21] The simplest organocatalyst, also the most common, is the amino acid proline.[22,23] The origins of organocatalysis date back to 1912, when Bredig and Fiske used alkaloids quinine and quinidine to accelerate the reaction of hydrogen cyanide, HCN, and benzaldehyde. Even though the resulting cyanohydrins were optically active and of opposing chirality, optical yields below 10% ee were obtained.[24] Ground-breaking work was done by Pracejus et al. in the 60s, using alkaloids as a catalyst for the addition of methanol on 1-methyl-1-phenylketene, resulting in 74 %ee (Figure 5).[25,26]

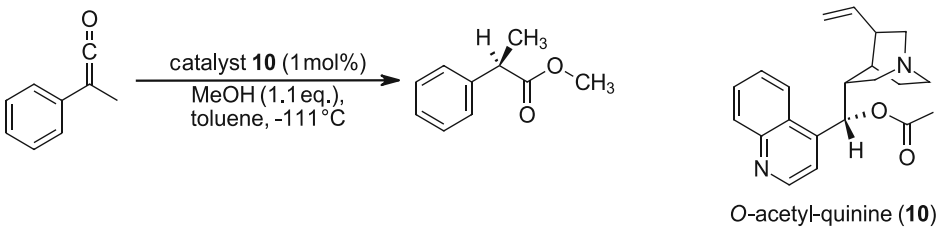

O-acetyl-quinine (**10**)

Figure 5: Alkaloid catalysed reaction of 1-methyl-1-phenylketene[25]

One decade later, further successful discoveries were reported, such as the Hajos-Parrish-Eder-Sauer-Wiechert reaction; a proline-catalysed intramolecular asymmetric aldol cyclodehydration of the achiral trione to the unsaturated Wieland–Miescher ketone. This particular ketone is an essential intermediate in steroid synthesis.[27,28] Even though the first discoveries of proline as a catalyst were made in the 70s, the catalytic potential of proline was deciphered much later. In 2000, List et al. reported further proline-catalysed reactions for *inter*molecular aldol reactions (Figure 6).[29,30] The Nobel Prize in Chemistry was awarded to List and MacMillan in 2021 for their contribution to asymmetric organocatalysis.

In general, organocatalysis can be classified into two major groups; “covalent” and “non-covalent” catalysis. As their name suggests, organocatalysts can either form covalent adducts with the substrates or utilise non-covalent interactions such as hydrogen bonds or ion pairs, which fall under the category of non-covalent catalysis.

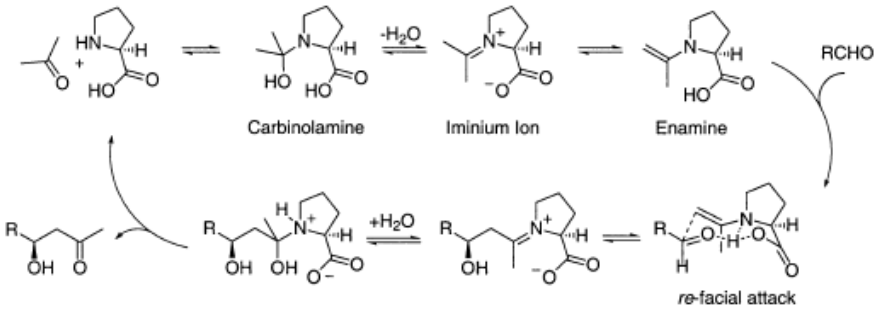

Figure 6: Originally proposed mechanism of the proline-catalysed direct asymmetric aldol reaction as an example of a covalent activation mode[30]

The covalent activation mode includes amino catalysis (including enamine catalysis, iminium catalysis, SOMO catalysis), and carbene catalysis (e.g., NHCs). For non-covalent catalysis (Figure 7), the formation of hydrogen-bonded adducts between substrate and catalyst or on protonation/deprotonation seems to be majorly occurring.[17]

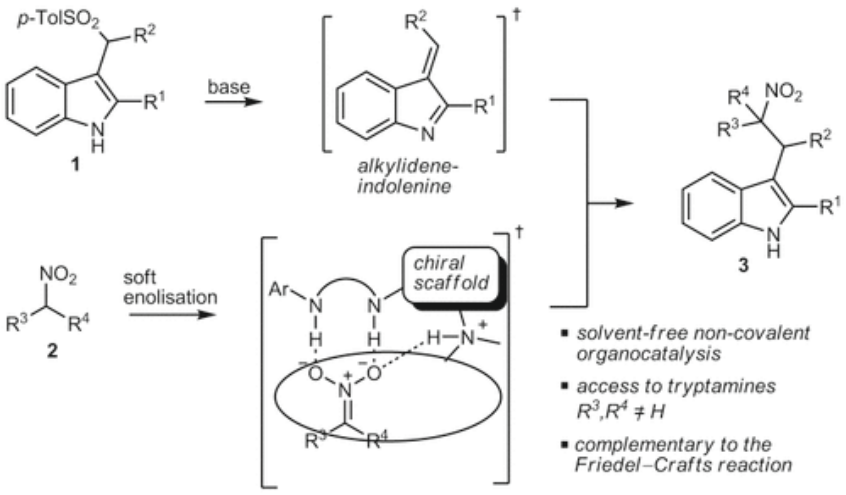

Figure 7: Example of non-covalent catalysis: Catalytic addition of nitroalkanes to alkylidene indolenines[31]

1.3.1 Enamine Catalysis

The concept of enamine catalysis is based on the mechanism of aldolases, which are enzymes involved in the metabolism of fructose-1,6-biphosphate. In aldolase catalysis, the amino acid lysine forms an enamine intermediate with the ketone or aldehyde substrate, leading to the formation of the desired intermediates, i.e., dihydroxyacetone phosphate (DHAP) and glyceraldehyde-3-phosphate (G3P).[32] Also, enamine catalysis is mainly applied for aldol reactions, which enable the construction of building blocks for structurally complex molecules. In aldol reactions, both nucleophilic addition and enolization occur. Lewis and Brønsted acids and bases can catalyse the aldol reaction, as nucleophilic addition is facilitated by acid catalysis, while either acids or bases catalyse enolization.[33,34] Natural aldolases use both acids and bases on their active site for the catalysis of aldol reactions. Class I aldolases rely on the Lewis base catalysis of a primary amino group (Figure 8), for instance, lysine. This is not compatible with living organisms since acidic or basic conditions would be detrimental to healthy cells. In order to overcome this limitation, aldolases decrease the pK_a of the carbonyl donor by converting the donor into an iminium ion (**A**). In enamine catalysis, a weak Brønsted acid thus acts as a co-catalyst to facilitate the deprotonation step, leading to the enamine intermediate's formation (**B**). Addition of the carbonyl acceptor leads to the formation of another iminium species (**C**). The amine catalyst is regenerated *via* hydrolysis, whereby the aldol product (**D**) is released.[35,36]

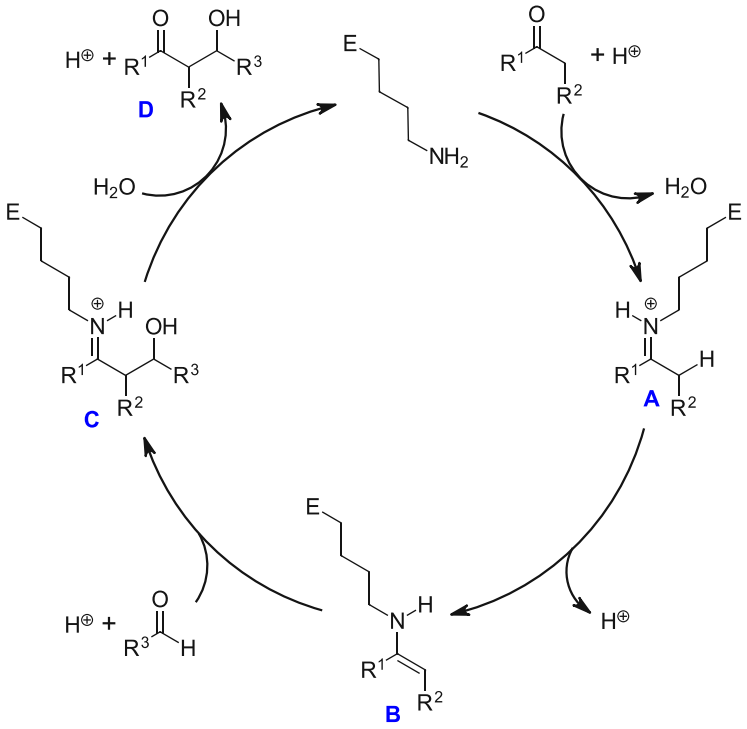

Figure 8: Mechanism of aldolases via enamine catalysis

Enamines are unsaturated compounds formed by carbonyls and secondary amines. They are labile and, therefore, quite valuable for organic chemistry and nature. The name “enamine” was established by Wittig and Blumenthal in 1927,[37] yet the first synthesis of an enamine compound was reported in 1936 by Mannich and Davidsen.[38] Only later, in the 1950s, enamines gained attention for various synthetic applications such as alkylations by Stork et al.[39–41] For a long time, investigations have focused on enamines as intermediates and tools for specific mono-substitution reactions of ketones and aldehydes. The peculiar property of enamines is their lability due to the HOMO elevating effect and the resulting increase in reactivity with electrophiles in the α-position. The n, π-conjugation of the amino group of the formed enamine with the C=C double bond increases the electron density on the carbon atom at the β-position. Consequently, the enamine is accessible to electrophiles under mild or neutral conditions. Furthermore, enamines can reversibly form ammonium salts, leading to iminium compounds (Figure 9). Further steps can be the electrophilic substitution of enamines derived from ketones by selective mono-alkylation or -acylation. Ketones, resulting from the hydrolysis of the intermediate iminium salt or the isolable substituted enamine, if R^4 is hydrogen, are ultimately formed. These mechanisms also apply to the catalytic cycle of enamine catalysis. Depending on the class of electrophile, two mechanisms are feasible.[42]

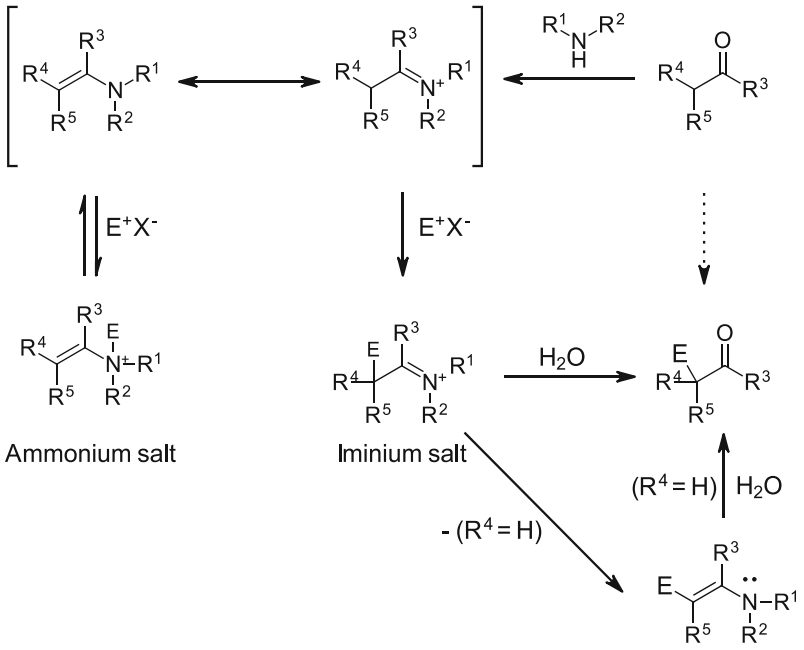

Figure 9: Mechanism of enamine formation

One possible pathway is the insertion of a double bond containing electrophile (e.g., aldehydes, imines, Michael acceptors) into the α-C–H bond of the carbonyl compound *via* "nucleophilic addition" (Figure 10, left). The other pathway, where a single bond electrophile (e.g., alkyl halides) is attacked, also leading to a stoichiometric alkylated product, is called "nucleophilic substitution" (Figure 10, right).[22]

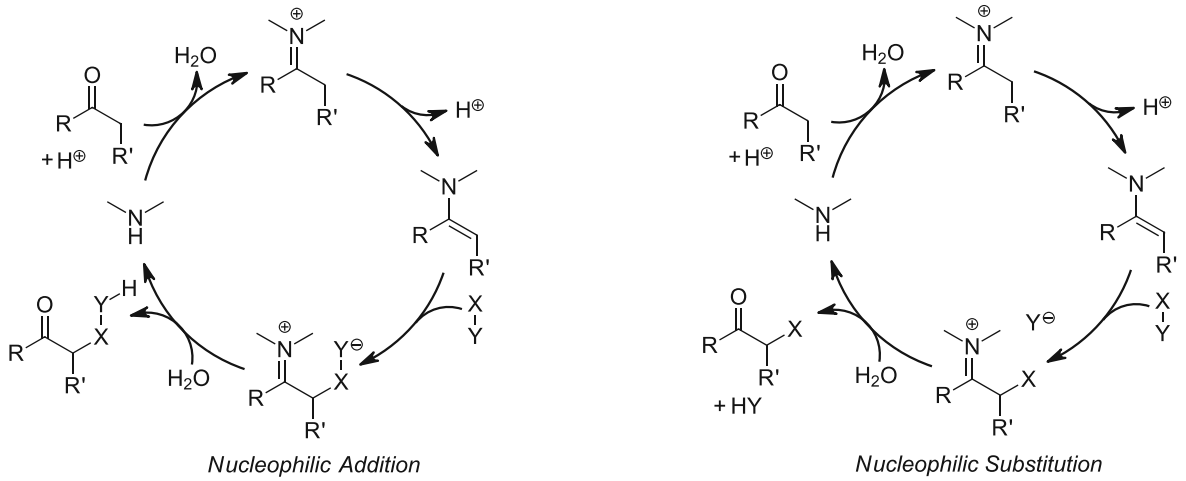

Figure 10: Two mechanism paths of enamine catalysis

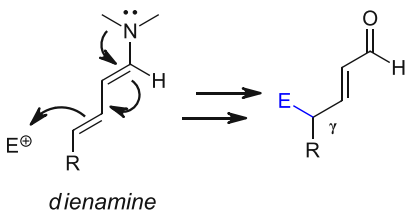

Figure 11: Asymmetric γ-functionalization via enamine catalysis

The mechanistic principle of, enamine catalysis is applicable to a broad range of reaction types, such as Mannich and Michael reactions, and the asymmetric α-and γ-functionalisation of carbonyl compounds (Figure 11). Ultimately, a large pool of catalytic transformations, as shown in Figure 12**,** is feasible.

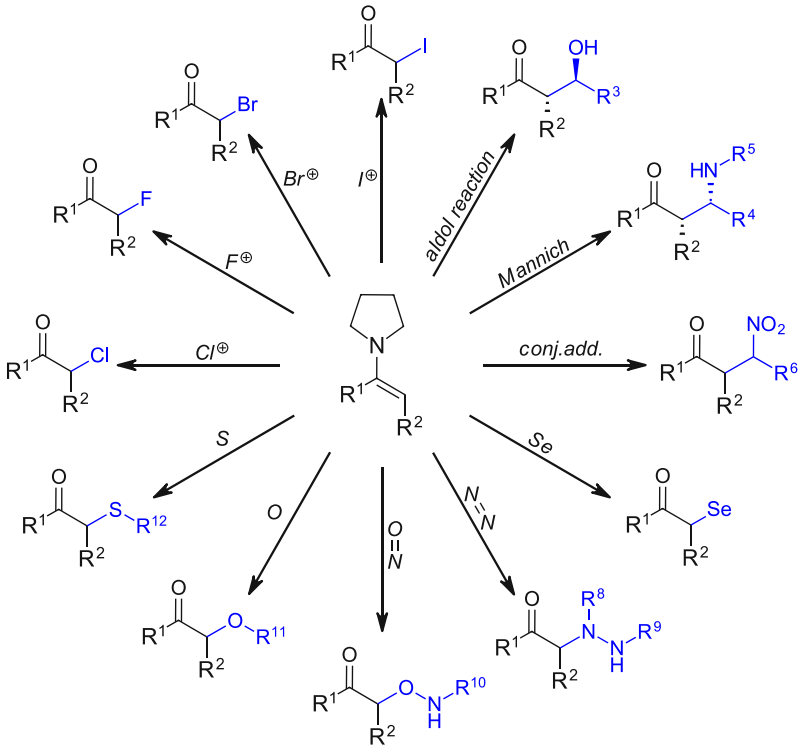

Figure 12: Scope of enamine catalysis

1.3.2 Iminium Catalysis

The operational simplicity is a significant advantage of amine catalysis. The reason is that the intermediate, formed by chiral secondary amines, and the substrate, are tolerant towards moisture and oxygen. Therefore, while an inert atmosphere and dry solvents are not required, rendering the experimental work fast and simple.[43]

As the name already indicate, substrates can be converted into products by forming an iminium intermediate with an amine catalyst. In general, the condensation of aldehydes or ketones with primary amines results in an equilibrium containing many imines.[44,45] Iminium compounds can be formed with primary amines and isolated as salts with the assistance of strong acids. This also applies to secondary amines that are preferentially used in iminium catalysis.

The amino catalyst affords/accesses the ketone or aldehyde by forming the iminium species, which is more electrophilic than the carbonyl compound, hence more vulnerable towards nucleophilic attack. The mechanism of iminium-ion formation is similar to one of enamine catalysis, even though there are

different types of nucleophile-electrophile interactions (Figure 13), including cycloadditions, nucleophilic additions, attacks by bases (leading to deprotonation and formation of enamine) and retro aldol-type processes (e.g., decarboxylation).[23]

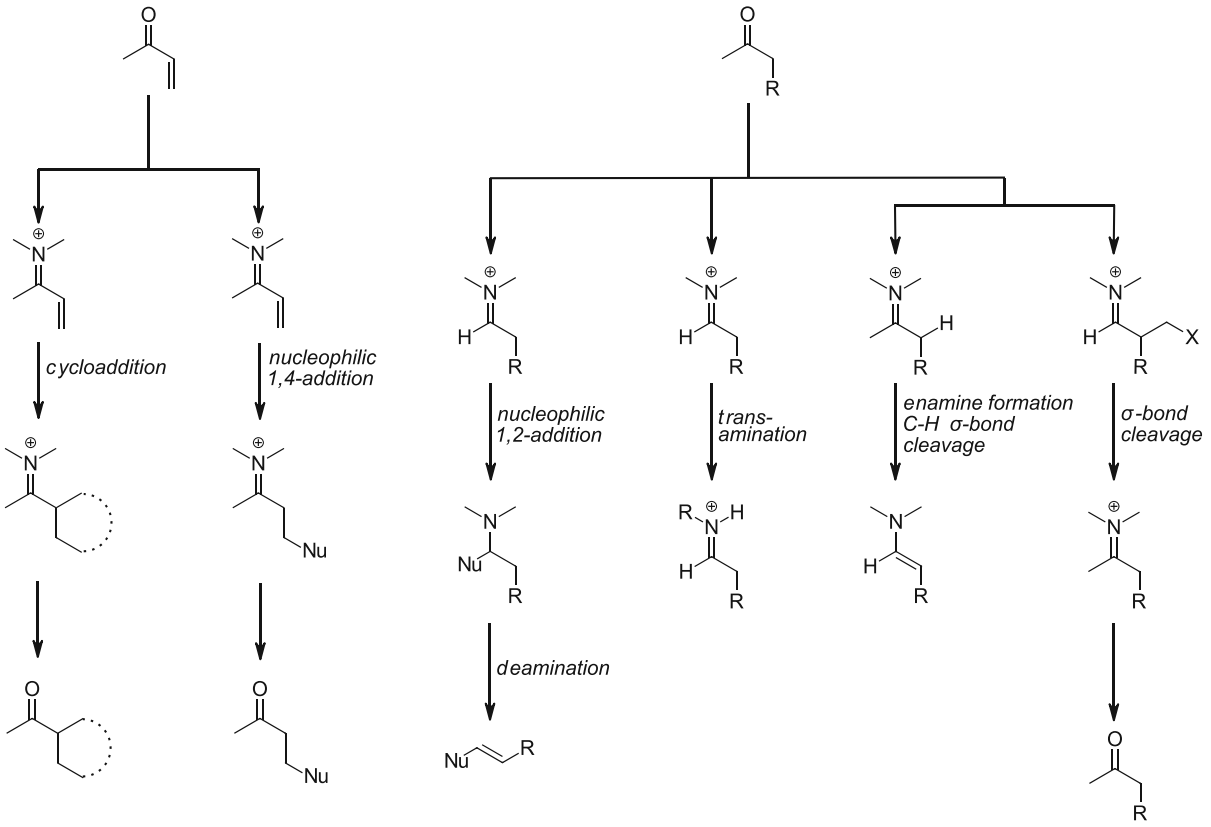

Figure 13: Examples of possible modes of iminium activation

An iminium-activated reaction is not necessarily iminium-catalysed as well. If the amine catalyst is released in the final hydrolysis or elimination step, then the iminium-activated reaction is also iminium-catalysed. However, the nucleophilic addition of a hydride ion to a C=N double bond is categorised as an iminium–activated reaction due to the formation of an iminium intermediate. Yet, it cannot be considered iminium-catalysed since the amine becomes trapped in the reduction step. There is no definite year of the discovery of iminium catalysis, but evidence suggests that the concept of iminium catalysis has existed since the 19th century. For example, Knoevenagel discovered a family of iminium-catalysed condensation reactions starting in 1894.[46,47] The first proof of concept involving iminium ions as active intermediates was reported in 1907 by Pollak in the decarboxylation of β-ketocarboxylic acids.[48] It was discovered that the decarboxylation of acetoacetic acid can be catalysed by two proteins, albumin and casein, in the presence of various amino acids and ammonium salts. Widmark and Jeppsson performed an analogous reaction with aniline in 1922, where they determined an optimal pH of 3 and 4 for this reaction.[49] Further research by Pedersen proposed an iminium activation of amine-catalysed decarboxylation of β-ketoacids.[50,51] Other considerable discoveries of iminium

catalysis have been reported in the field of transamination[52], deprotonation reactions,[53,54] and recently also Diels-Alder reactions, with MacMillan and co-workers performing enantioselective iminium catalysis. Additionally, MacMillan coined the term “LUMO-lowering catalysis” to describe the iminium catalysis concept in 2000 (Figure 14).

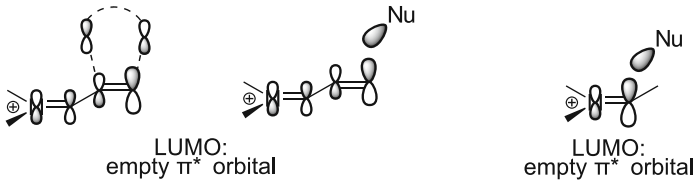

Figure 14: Depiction of iminium catalysis using orbital schemes

Precisely, the strategies of (i) LUMO-lowering activation and (ii) the kinetic lability towards substitution, which both occur in Lewis acid catalysis, were studied for iminium catalysis.

MacMillan’s catalyst (Figure 15, left) enables enantioselective iminium catalysis for a broad range of processes, such as the Diels-Alder reaction.[55] In addition to imidazolidinone catalysts, substituted pyrrolidines are also known to be as efficient as iminium catalysts.[56]

Figure 15:Structure of first-generation MacMillan catalyst (left) and diarylprolinol silyl ether (right)

Proline and its derivatives, such as diaryl prolinol silyl ethers (Figure 15, right), are favoured catalysts for ring-forming, domino reactions. They were discovered by the groups of Jorgensen[57] and Hayashi[58] and have gained broad attention, even though secondary amines are otherwise less favourable. However, they show great activity for α-substituted enals as substrates. Other successful catalysts are aromatic amines, diamines (e.g., BINAM, Figure 16, left)[59,60] and chiral triamine (Figure 16, right)[61] for the Diels–Alder reaction. Additionally, the enantioselectivity of iminium-catalysed reactions can be directed by chiral counteranions through contact ion pairing with the iminium cation.[62,63]

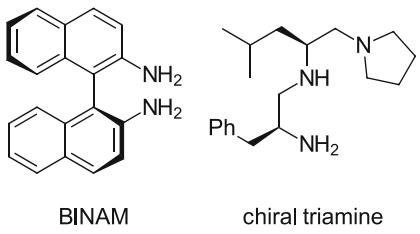

Figure 16: Example of two organocatalysts, BINAM (left) and a chiral triamine (right)

1.3.3 Conjugate Additions

Conjugate additions, or 1,4–nucleophilic additions, are additions to α,β-unsaturated carbonyl compounds. Generally, simple alkene compounds show no polarity at the 1,2-position. Hence, they are unreactive. However, electron-withdrawing substituents, such as carbonyls, render the C–C double bond active in this position, thus making it vulnerable to nucleophiles. The β-position of the carbonyl compound acts as an electrophile, enabling reactivity with nucleophiles. The negative charge shifts to the oxygen of the carbonyl, forming an alkoxide ion. Consequently, the oxygen is acting as a reservoir for the negative charge. Two famous conjugate additions are the Stork enamine reaction and the Michael addition.[64]

1.3.4 Michael Addition

As mentioned above, the Michael addition is the addition of the enolate of a ketone (the Michael donor) to an α,β-unsaturated carbonyl compound (Michael acceptor), leading to a 1,5-dicarbonyl compound (Michael adduct). Figure 17 provides a schematic overview of the Michael addition. The Michael acceptor requires an electron-withdrawing group, such as an acyl or nitrile group, to make the β-carbon accessible to nucleophilic attacks.[65] The best Michael donors are enolates with two electron-withdrawing groups, for example, β-diketone, β-diester, β-ketoester and β-ketonitriles. The Michael addition proceeds *via* a mechanism in which the Michael donor is deprotonated by a base, generating a carbanion that can attack the Michael acceptor in the β-position. Nucleophiles can also react with β-unsaturated esters and amides due to the relatively low reactivity of the carbonyl group in these compounds. The resulting enolate intermediate is subsequently reprotonated by the protonated base.[64]

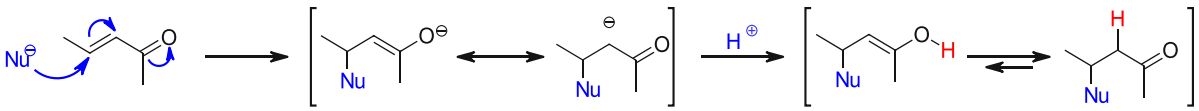

Figure 17: Schematic overview of Michael Addition

In recent years, asymmetric Michael additions have gained significant attention, enabling the enantioselective synthesis of optically pure compounds, such as warfarin. Asymmetric Michael addition has, thus, expanded the application scope of warfarin, allowing for better customisation of dosage and treatment for patients based on their clinical profiles.[66]

1.3.5 SOMO Catalysis

To widen the scope of organocatalysis, different activation modes have been developed. The counterpart of enamine and iminium catalysis is SOMO catalysis, i.e., *single-occupied moleculare orbital* catalysis. In this activation mode, an enamine catalyst participates as a reactive 3π-electron radical cation, making it an electrophile and reactive towards weakly nucleophilic carbon-based

reactants at the α-position (Figure 18).[67] Further research proved the importance of one-electron oxidants to achieve successful results and enantioselective transformations, indicating their potential to act similarly enamine catalysts. Additionally, SOMO catalysis can be applied for α-allylation[68], α-vinylation[69] and α-enolation[70] of aldehydes, thus enabling reactions that can be realized neither by enamine nor iminium catalysis.

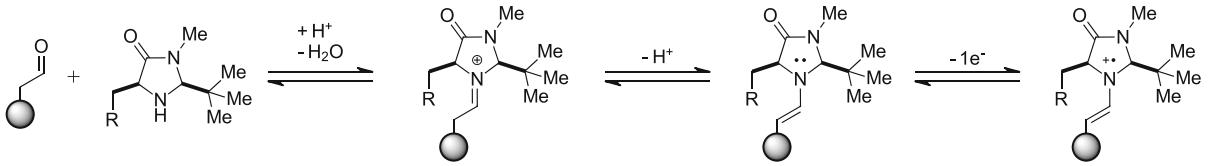

Figure 18 Organocatalytic activation modes in chiral amine catalysis[67]

Initially, the main goal was the direct asymmetric α-alkylation of aldehyde **5** (**Figure 19**). Trials with other concepts, such as reactive α-alkylation agents, would constitute an obstacle due to the low reactivity of the enamine towards alkylation agents. This results in low conversion and undesired side reactions, such as aldehyde self-dimerization and/or catalyst alkylation. SOMO catalysis offers a workaround to overcome this obstacle to enable the direct asymmetric α-alkylation of aldehyde **5**. A 2nd generation MacMillan catalyst was developed for the SOMO activation mode, forming the enamine with the aldehyde first (Figure 20). To generate the SOMO intermediate, a selective single electron transfer oxidant, i.e., a metal salt oxidant such as ceric(IV) ammonium nitrate (CAN), has to be introduced to the enamine, forming **4a**. The reactant **8** can attack **4a** from the *Si*-face, forming an enantioselective C-C bond formation in the α-position (where the SOMO orbital coefficient is the highest), leading to **9a**. The resulting β-silyl radical undergoes a second single electron transfer, initiated by a second CAN molecule to form the stable β-silyl cation **10a**. β-Silyl elimination reforms the double bond, and hydrolysis releases the product while the imidazolidinone catalyst **1a** is regenerated.

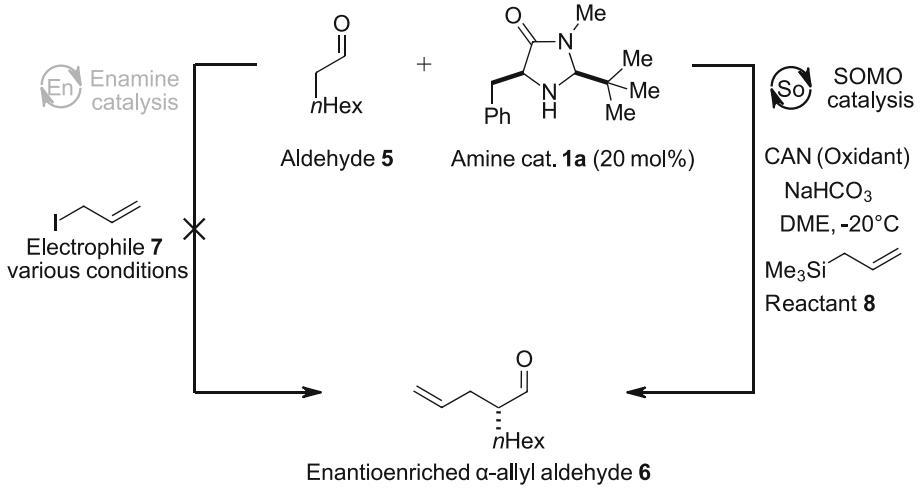

Figure 19: Catalytic enantioselective α-alkylation of carbonyl compounds[67]

The concept of SOMO catalysis has made the essential direct asymmetric α-alkylation of the aldehyde feasible. Acceptors of electrophilic radical cation, such as electron-rich silyl enol ethers, vinyl trifluoroborate salts and silyl nitrates, are suitable reactants with remarkable reactivity with the intermediate, leading to good yields and high enantiomeric excess.[67]

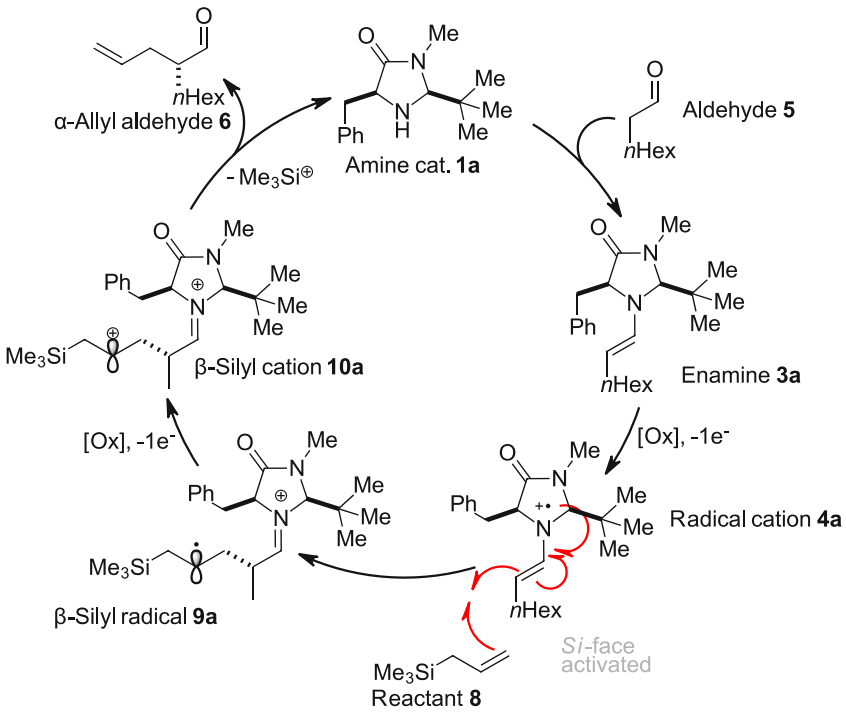

Figure 20: Catalytic Cycle of organo-SOMO catalysis[67]

All these reactants have a common feature: a "built-in" silicon- or boron-based leaving group for easier elimination after the second oxidation step. However, SOMO catalysis is not limited to aldehydes only but applies to ketones. This requires modified imidazolidinone catalysts, and further cascade reactions such as a formal [4 + 2] cycloaddition with a simple aldehyde and styrene were made feasible by using noncoordinating counteranion oxidants (e.g., $Fe(phen)_3(SbF_6)_3$). Ultimately, SOMO catalysis is not limited to C–C bond formation but is also applicable to the formation of carbon-halogen bonds or polyene cyclisation of polyenals. Even though it was developed for direct asymmetric α-alkylation, the scope of SOMO catalysis nowadays offers an elegant way to synthesise valuable synthons, such as tetrahydrofuran or lactone products.[67]

1.4 Homogeneous *versus* Heterogeneous Catalysis

Catalysts can be categorised into two groups: homogeneous and heterogeneous catalysis. In the case of heterogeneous catalysis, the substrates and the catalysts are in different aggregation phases (Figure 21, top). For example, the reagents are in the gaseous state, while the catalyst is in the solid state. The Haber-Bosch process is a representative example of heterogeneous catalysis, where the nitrogen and hydrogen substrates are gaseous, while the α-Fe catalyst is solid.[71–74]

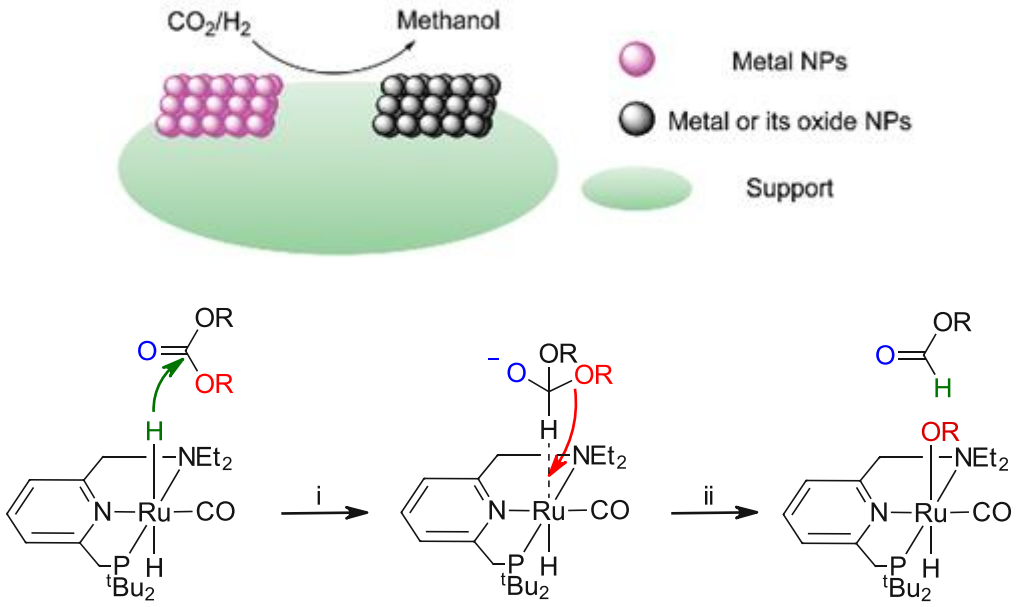

Figure 21: Example of heterogeneous catalysis (top) and homogeneous catalysis (bottom)[75]

On the other hand, when reagents and catalysts are in the same phase, then the process is categorised as "homogeneous catalysis" (Figure 21, bottom). A significant example is displayed in cells of living organisms, where enzymes that act as the catalyst and the substrates are dissolved in the same aqueous phase. Catalytical processes can be roughly classified into biocatalysis, metal (organic) catalysis, and organocatalysis (Figure 22).

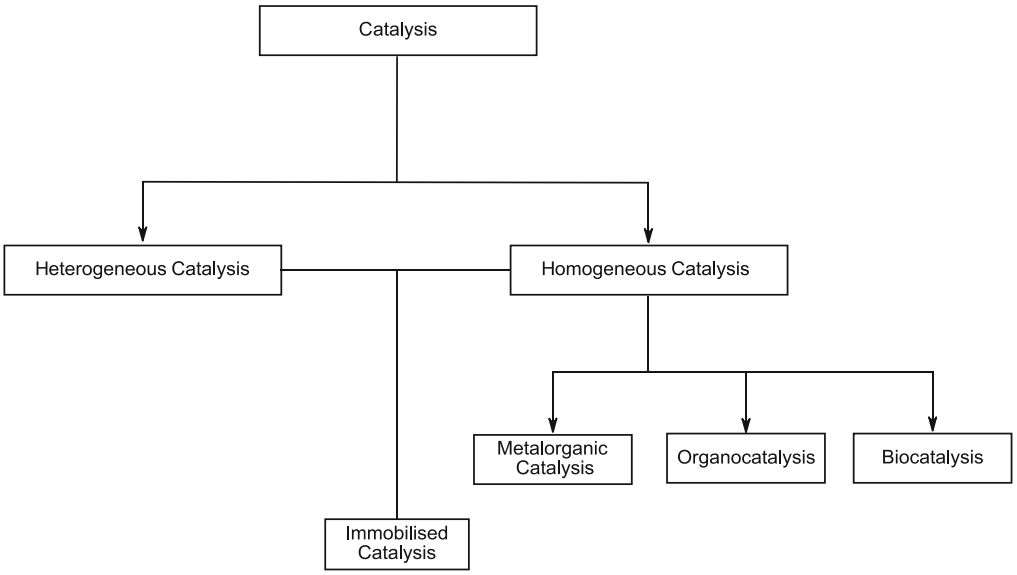

Figure 22: Classification of catalytical processes

Both homogeneous and heterogeneous catalysis have advantages and disadvantages (Table 1). Heterogeneous catalysts are usually solid materials, especially metals or metal atoms attached to a ceramic support. Heterogeneous catalysis involves no phase miscibility between the reagents and the

catalyst and the employed catalysts have high thermal stability, thereby allowing reactions with higher temperatures, as in the Haber-Bosch process.

Table 1: Advantages and disadvantages of hetero- and homogeneous catalysis

	Homogeneous catalysis	Heterogeneous catalysis
Advantage	• Efficient heat transfer • High selectivity • Diffusion-controlled • Often very high rates	• Easy and inexpensive separation • High thermal stability • High surface area • Long life
Disadvantage	- Elaborate separation - Low thermal stability - Expensive and challenging to recycle	- Problematic heat transfer - Low selectivity - May be diffusion controlled

Conversely, the reagents and catalysts exist in the same phase in homogeneous catalysis. Homogenous catalysts show efficient heat transfer. They allow stereo-selective synthesis of compounds by optimising the catalyst's features. Also, some catalysts need a co-catalyst, e.g., enzymes or in hydroxylation of alkenes, osmium (VIII)-tetroxide. Another disadvantage, in comparison to heterogenous catalysts, is their difficult recovery.

Despite the numerous advantages associated with catalyst immobilisation, certain drawbacks, such as the need for extra steps, catalyst modification, low selectivity and the reduction of catalytic activity exist, still remain to be addressed.

1.5 Immobilisation

The immobilisation of homogeneous catalysts facilitates the implementation of continuous flow processes, which is highly desirable in the industry due to its efficiency and consistency in chemical input and output, without interruption for adding or transferring ingredients as is required in batch processes. A significant advantage of heterogeneous catalysis is the ease of separation, since the catalyst and reaction media are in different phases, the heterogeneous catalyst offers simple separation, such as filtration, centrifugation, or decantation. Several parameters influence the properties and potential application of immobilised catalysts. The effectiveness of the heterogeneous catalysts depends not only on the physicochemical nature, porosity, and dimensions of the support but also on the density of the catalytic sites and the nature and length of the spacer between the catalytic sites and the surface of the matrix.

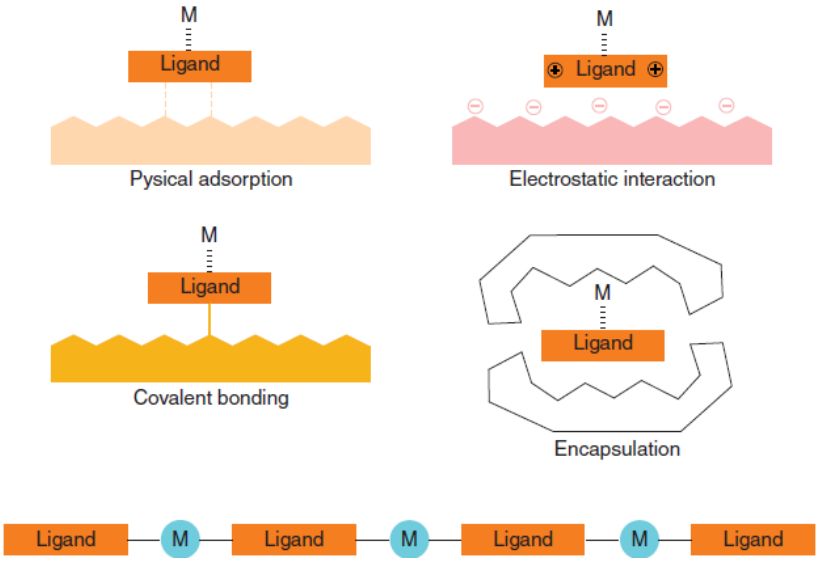

Figure 23: Methods for the immobilisation of catalyst onto solid supports[76]

The immobilisation of catalysts onto support materials can be achieved with three different mechanisms: (i) covalent bonding (chemisorption), (ii) non-covalent bonding (physisorption) and (iii) encapsulation (**Figure 23**). The most significant advantage of chemisorption is that it minimizes the possibility of catalyst leaching off the solid support, since the catalyst is attached covalently on the surface of the support material, however to the expense of catalytic activity and enantioselectivity. In physisorption, the catalyst is adsorbed onto the surface of the support material through hydrogen bonding, electrostatic interactions, or van der Waals forces and, typically, only experiences minimal loss in catalytic activity or enantioselectivity. However, leaching constitutes a significant issue due to the strong dependence between the catalyst, support material, and solvent. Electrostatic interactions are stronger; hence, leaching is an issue in this method. In the case of is immobilisation *via* encapsulation, the catalyst is physically trapped inside the pores or cavities of the support material.[76]

1.5.1 Immobilisation on Silica

Silica is a versatile material with a wide range of applications. While it is essential in laboratory settings, particularly for chromatography, silica has also demonstrated its significance for commercial purposes. Its particle size can be adjusted, allowing for a diverse range of separation efficiencies. Silica is extremely hygroscopic, making it an applicable drying agent for several commercial items, such as shoes. Silica has also gained much attention as support material for the immobilisation of catalysts due to its inertness, and remarkable thermal stability. Silica supports are usually synthesised *via* sol-gel process. As mentioned above, its adjustability facilitates the preparation of particles in different shapes and sizes and offers excellent control over the properties of the final product. Its versatility enables the immobilisation of organo- and organometallic catalysts on several silica-based supports, ranging from xerogels and aerogels to mesoporous silica,[77,78] periodic mesoporous organosilica (PMO),[79]

silica nanoparticles,[80] microcapsules,[81] and nanospheres.[82,83] The catalyst can be immobilised *via* chemisorption, electrostatic interactions, or silica microencapsulation. In the case of chemisorption, the catalyst is post-synthetically attached to the pre-treated silica surface (Figure 24).

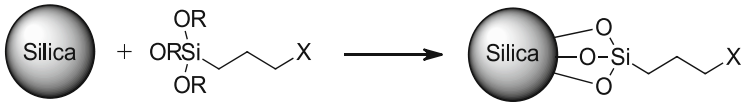

Figure 24: Example of surface treatment on silica with modified catalyst

Other possible support materials for the catalyst are (i) polymers (e.g., dendrimers), (ii) metalorganic frameworks, (iii) periodic mesoporous organosilicas, (iv) membranes and (v) magnetic nanoparticles. Due to a lower surface area-to-volume ratio, the catalyst usually lacks catalytic activity in silica and polymers compared to their counterparts. The latter examples (ii)–(v) offer a solution to this problem because of their high surface area.[76]

2 Aim of the thesis

Michael's addition plays a significant role in the synthesis of different drugs and natural products. One of those drugs is warfarin, which is synthesised by the Michael addition of benzylideneacetone and 4-hydroxycoumarin. Both enantiomers show anti-coagulative effects, which is a great advantage. Further studies have shown that the effectiveness of the (*S*)-enantiomer is higher than of the (*R*)-enantiomer. With asymmetric iminium catalysis, warfarin can be synthesised in an enantioselective manner, thereby enabling a better adjustment to the severity of the coagulation.

The thesis aims to facilitate and concentrate on the response of cyclic enones with diverse Michael donors through iminium catalysis, utilising diamines derived from amino acids. The focus is developing an economical catalyst system that can be ideally synthesised from amino acids and exhibits excellent enantioselectivity (ee) and yield. The overall goal is broken down in 5 strategic steps, as shown in Figure 26.

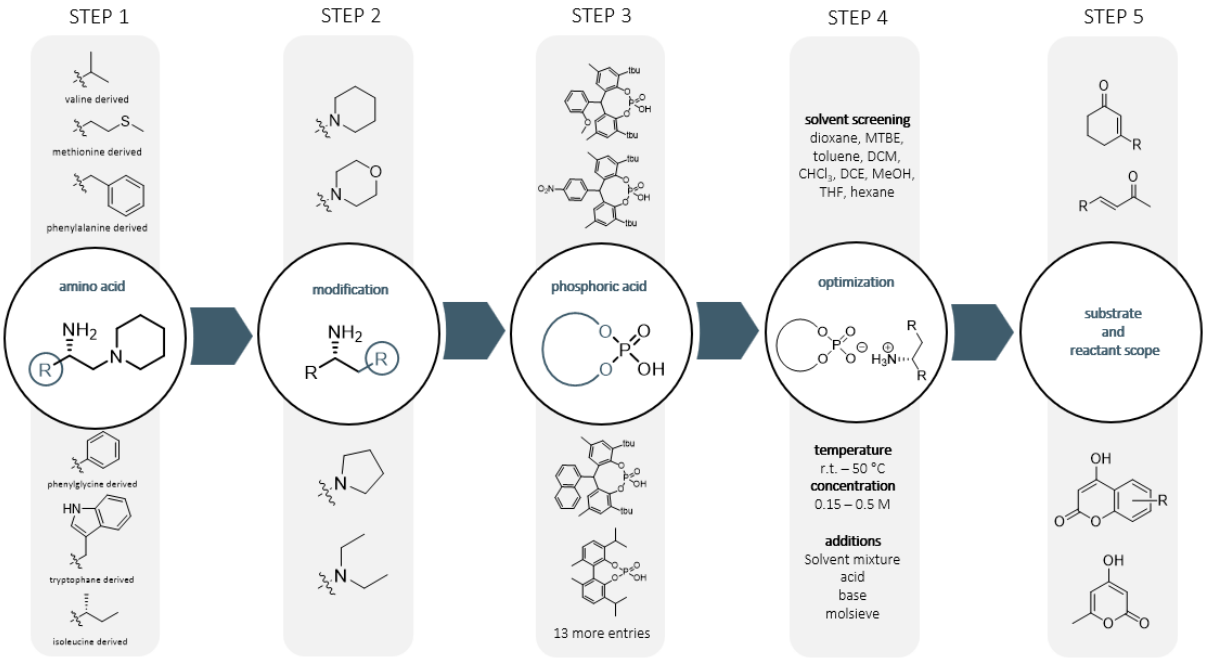

Figure 25: General overview of our project

Another goal was to investigate the immobilisation of our catalyst on a solid support material, enabling further applicability for continuous-flow chemical reactions and, ultimately, uninterrupted conversion of substrates to the desired product. The primary challenge in continuous-flow chemistry is to maintain the catalytic activity and enantioselectivity. Various approaches involving physisorption and chemisorption were explored to overcome this and other issues.

3 Results and Discussion

The catalytic system initially contained a diamine and a phosphoric acid. Later investigation showed that trifluoroacetic showed better results. During the optimisation process, various diamines were used, each synthesised from different amino acids as the starting material and other amines for the coupling step.

3.1 Optimisation

3.1.1 Screening of the Side-Chain Functionality

This project aimed to investigate whether amino acid-derived diamines, in conjunction with chiral phosphoric acid, could catalyse the synthesis of warfarin and its derivatives. Our research focused on the Michael addition reaction of cyclic enones, precisely the reaction between 2-cyclohexen-1-one and 4-hydroxycoumarin, as there was limited existing literature on this topic. Even though some organo-catalysts have been reported for the synthesis of warfarin[8,12,66], several diamines were tested in our research because of their cost efficiency and synthetic simplicity. The phosphoric acid acts as a counteranion, enhancing the reaction's enantioselectivity. Also, previous experiments showed an excellent catalytic activity of this system, i.e., diamine plus phosphoric acid, with other reactions. The amino acid's N-terminus and sidechain remain intact during the synthesis, while a secondary amine substitutes the carboxylic acid. At first, a proof-of-concept reaction with 2-cyclohexen-1-one and 4-hydroxycourmarin was performed. A diamine from phenylglycine and phosphoric acid **12** was used and the results showed catalytic activity (34%) and good enantioselectivity (89% ee). With that knowledge at hand, as a first optimisation step, variation of the diamine sidechains was evaluated. As the tertiary amine, piperidine was used. The results are shown in Table 2. Based on the data, the phenylglycine-derived diamine had the lowest conversion rate at 34%. However, it demonstrated the highest enantioselectivity with 89% ee. The results show that a sterically demanding group on the carbon atom, next to the primary amine, significantly impacts the enantioselectivity and conversion in this reaction. Even though the conversion in entries 2-6 was relatively higher than in entry 1, diamine **1** was chosen for further optimisation since it showed the highest enantioselectivity.

Table 2: Results of sidechain-screening

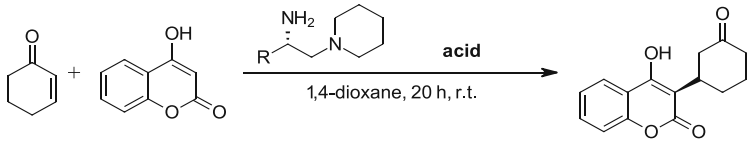

entry[a]	diamine	acid	acid eq.	conv. [%][b]	ee [%][c]
1	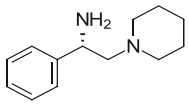 1		1.1	34	89
2	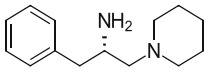 2		1.1	77	67
3	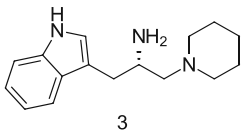 3	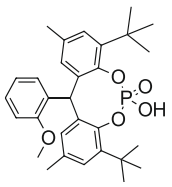	1.1	97	66
4	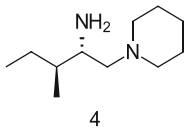 4		1.1	89	67
5	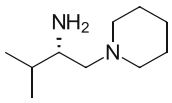 5		1.1	95	74
6	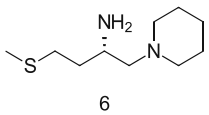 6		1.1	77	64

[a]Performed with 0.16 mmol ketone, 0.17 mmol 4-hydroxcoumarin, 10 mol% diamine and 10 mol% acid in 0.7 ml solvent at r.t. for 20 h [b]Determined by GC-MS, [c]Determined by HPLC

3.1.2 Screening of the Tertiary Amine Moiety

Since the tertiary amine is essential for the transformation of the reactant to the substrate, different tertiary amine moieties were used to investigate whether the conversion and enantioselectivity change. As the counteranion, phosphoric acid **12** was chosen again. Table 3 shows the results of the screening. The highest conversion was achieved with diamine **7**, and even the enantioselectivity was relatively high, with 87% ee. All the diamines showed similar enantioselectivities. Only diamine **9** was an outlier with 5% conversion and 77% ee. Even though diamine **7** had the best conversion and the second-best ee-value, diamine **1**, which showed the best enantioselectivity, was selected since the conversion is more straightforward to enhance than the enantioselectivity. It also has a financial

benefit since the synthesis of diamine **1** requires piperidine, the cheapest among all the secondary amines used for coupling. Nevertheless, a significant disadvantage of piperidine is its toxicity.

Table 3: Results of sidechain-screening

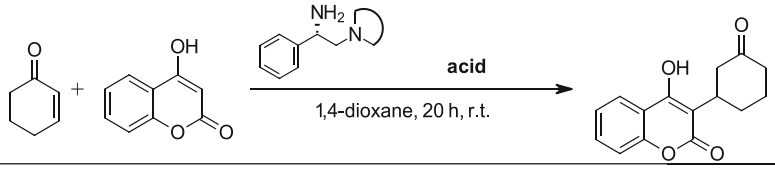

entry[a]	diamine	acid	acid eq.	conv. [%][b]	ee [%][c]
1	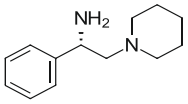 1		1.1	34	89
2	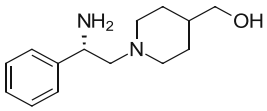 7		1.1	45	87
3	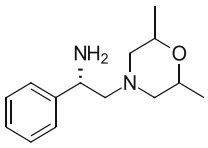 8	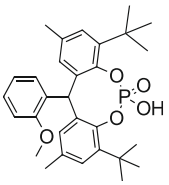	1.1	29	87
4	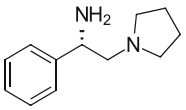 9		1.1	5	77
5	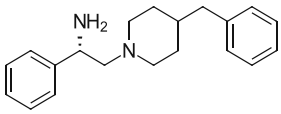 10		1.1	29	89
6	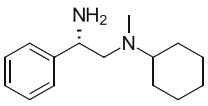 11		1.1	25	84

[a]Performed with 0.16 mmol ketone, 0.17 mmol 4-hydroxcoumarin, 10 mol% diamine and 10 mol% acid in 0.7 ml solvent at r.t. for 20 h [b]Determined by GC-MS, [c]Determined by HPLC

3.1.3 Screening with Different (Phosphoric)acids

After optimising the diamine, the focus shifted to the acidic part of the catalytic system. Different phosphoric acids, pentafluorobenzoic acid, and trifluoroacetic acid were investigated. The results in Table 4 demonstrate that the phosphoric acids have no significant impact on the enantioselectivity,

but the significantly influences the conversion. With phosphoric acid **20**, a conversion of 84% and 90% ee was achieved. Conversely, TFA showed the best enantioselectivity, which is unsurprising since Xie *et al*. report similar observations in vinylogous Michael addition, using TFA as an additive.[10] Therefore, TFA was selected for further optimisation. Compared to the phosphoric acids, TFA's huge advantages are its commercial availability, low price, and immediate use without prior modification. Yet, the phosphoric acids **17**, **22** and **20** are also worth mentioning. Especially phosphoric acid **20** shows remarkable enantioselectivity and the highest conversion out of all the other acids. Though **20** seems demanding and expensive to synthesise, the precursor is relatively cheap. Even though excellent results were attained, we still chose acid **21** for further optimisation because it is easier to increase the yield by modifying the reaction conditions, such as temperature, than increasing the enantioselectivity. Phosphoric acid **17** was also used to screen the enantioselectivity and conversion using different equivalents.

Table 4: Results of sidechain-screening

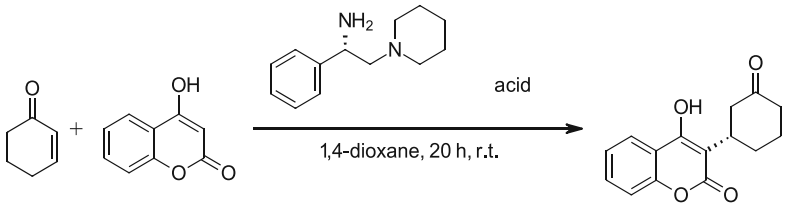

entry[a]	diamine	acid	Acid eq.	conv. [%][b]	ee [%][c]
1		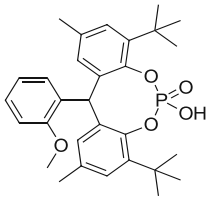 12	1.1	34	89
2	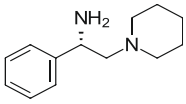 1	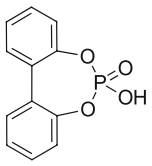 13	1.1	24	86
3		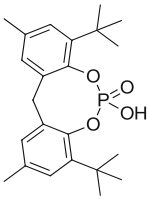 14	1.1	50	89

4		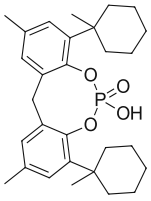 15	1.1	45	87
5		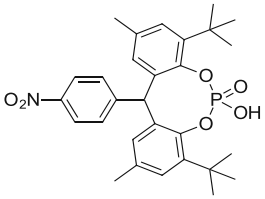 16	1.1	58	90
6		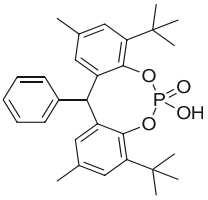 17	1.1	66	90
7		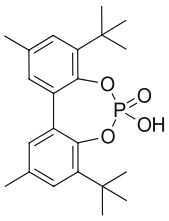 18	1.1	58	89
8	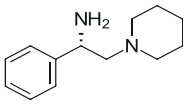 1	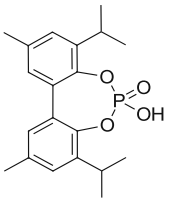 19	1.1	69	89
9		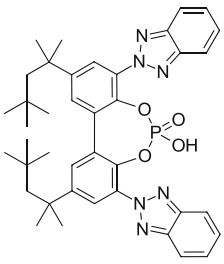 20	1.1	84	90
10		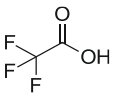 21	1.1	57	92
11		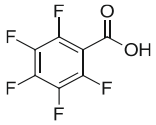 22	1.1	60	90

[a]Performed with 0.16 mmol ketone, 0.17 mmol 4-hydroxcoumarin, 10 mol% diamine and 10 mol% acid in 0.7 ml solvent at r.t. for 20 h[b]Determined by GC-MS, [c]Determined by HPLC

3.1.4 Equivalent Screening of Phosphoric Acid 17

To see if the conversion and especially the enantioselectivity change, using phosphoric acid, different equivalents of phosphoric acid **17** were used. Phosphoric acid **17** equivalents of 0.8, 1.3 and 1.8 were tested. A significant change in enantioselectivity and a dramatic change in conversion were observed, as shown in Table 5. The results indicate that 0.8 eq. of the phosphoric acid leads to a slight increase in enantioselectivity and conversion. Yet, the conversion decreases drastically with the increasing amount of **17**. Also, the enantioselectivity exhibits a significant decrease with increasing equivalents of the phosphoric acid. A similar behaviour is observed with TFA. The data demonstrates that the ratio between diamine and acid is crucial for the turnover of the reaction.

Table 5: Results of screening with phosphoric acid **17**

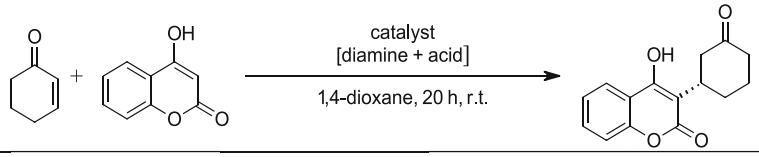

entry[a]	diamine	acid	acid eq.	conv. [%][b]	ee [%][c]	Δee[d]
1	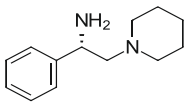 1	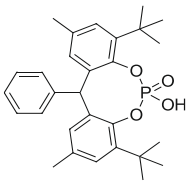 17	0.8	62	91	1
2			1.3	34	87	0
3			1.8	12	86	0

[a]Performed with 0.16 mmol ketone, 0.17 mmol 4-hydroxcoumarin, 10 mol% diamine in 0.7 ml solvent at r.t. for 20 h [b]Determined by GC-MS, [c]Determined by HPLC, [d]Δee is defined as difference between 1.0 eq. of acid and x eq. acid

3.1.5 Screening of Different Amounts of TFA

Since TFA showed the best results and is beneficial in terms of availability and price, it was used as the anionic counterpart for the reaction. Various equivalents of TFA were used, and a trial with no amount of the acid was performed, too, as shown in Table 6. The conversion, using only the amine, was 84%, yet there was a relative decrease in enantioselectivity to 36% ee. Compared to the reactions with an acid as a cocatalyst, this experiment proved the importance of an acidic counterpart for an enantioselective conversion of the ketone and 4-hydroxycoumarin. The other two entries showed that a deficit and an excess of TFA lead to a significant increase in conversion, compared to 1 eq. of TFA, although the enantioselectivity slightly decreased enantioselectivity decreased.

Table 6: Results of eq.-screening of TFA

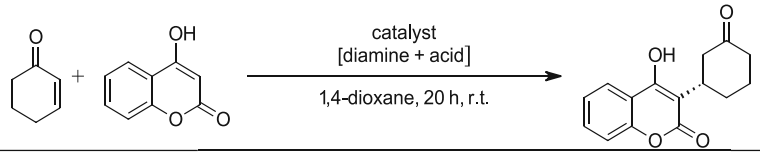

entry[a]	diamine	acid	TFA eq.	Conv. [%][b]	ee [%][c]	Δee[d]
1			0.0	84	36	0
2	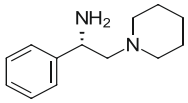 1	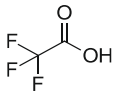 21	0.8	70	91	1
3			1.0	57	92	-
4			1.8	74	91	1

[a]Performed with 0.16 mmol ketone, 0.17 mmol 4-hydroxcoumarin, 10 mol% diamine in 0.7 ml solvent at r.t. for 20 h [b]Determined by GC-MS, [c]Determined by HPLC, [d]Δee is defined as difference between x eq. of TFA and 1.0 eq. TFA

3.1.6 Screening of Variable Water Content

After optimising the catalytic system, the influence of various amounts of water, ranging from 0.3 vol% up to 5.0 vol%, on the conversion and enantioselectivity was tested. The results in Table 7 show that already small amounts of water, from 0.3% to 1.0%, magnified the conversion significantly, and even the enantioselectivity increased from 93% ee up to 94% ee at 0.8 vol% and 1.0 vol%. Exceeding 1.0 vol% of water results in a significant decrease in conversion and a slight decrease in enantioselectivity to 91 % ee at 5 vol% of H_2O. This can be explained by the increase in the solution's relative permittivity (dielectric constant) when water is added. The increase in the dielectric constant inhibits the formation of the ion-pair of the catalytic amine, thereby decreasing the catalytic activity, which leads to a lower conversion. This also can be observed in section 3.1.9, where water was used as a solvent, whereas no conversion was observed. Since 1.0 vol% of water showed the best results in both, conversion (91%) and enantioselectivity (94% ee), further investigation was continued with 1.0 vol% H_2O.

Table 7: Results of water-screening

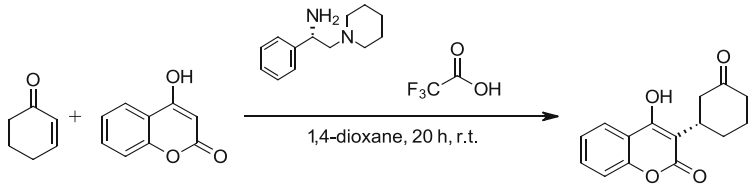

entry[a]	diamine	acid	water [vol%]	conv [%][b]	ee [%][c]	Δee[d]
1			0.3	90	93	1
2			0.5	88	93	1
3	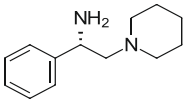 1	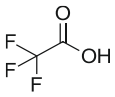 21	0.8	87	94	2
4			1.0	91	94	2
5			3.0	63	92	0
6			5.0	67	91	0

[a]Performed with 0.16 mmol ketone, 0.17 mmol 4-hydroxcoumarin, 10 mol% diamine and 10 mol% acid in 0.7 ml solvent at r.t. for 20 h, [b]Determined by GC-MS, [c]Determined by HPLC, [d]Δee is defined as difference between 0 vol% water and x vol% water

3.1.7 Optimization Using Pentafluorobenzoic Acid (PFBA) as an Additive

Additionally, different amounts of PFBA (5 and 10 mol%), as well as additional phosphoric acid 17 in the absence of PFBA were investigated. The results, shown in Table 8, indicate that 5 mol% and 10 mol% of PFBA affect the conversion and enantioselectivity. Overall, the enantioselectivity decreased in both cases to 93% ee. Yet, the conversion seemingly depends on the amount of PFBA being used; small amounts of PFBA reduce the conversion. Specifically, a significant decrease in conversion is observed, from 91% down to 85%, when PFBA is increased from 0 to 5 mol%. Surprisingly, the conversion rate increased with a higher amount of PFBA added. With 10 mol%, a conversion of 93% was achieved, while the addition of phosphoric acid **17** shows an influence in the conversion without a concurrent change in enantioselectivity. With all the data obtained, further optimisation was pursued without additional acid since no improvement was observed in its presence.

Table 8: Screening of additional PFBA (entry 1 & 2), phosphoric acid 17 (3) and no acid (4)

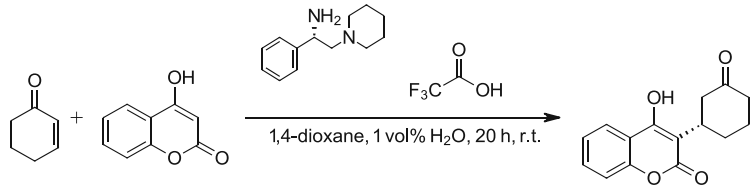

entry[a]	additional acid	add. acid [mol%]	conv. [%][b]	ee [%][c]	Δee[d]
1	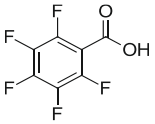 22	10	93	93	0
2		5	85	93	0
3	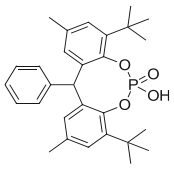 17	5	86	94	0
4	-	0	91	94	0

[a]Performed with 0.16 mmol ketone, 0.17 mmol 4-hydroxcoumarin, 10 mol% diamine and 10 mol% acid in 0.7 ml solvent at r.t. for 20 h, [b]Determined by GC-MS, [c]Determined by HPLC, [d]Δee is defined as difference between 0 mol% additional acid and x mol% additional acid

3.1.8 Trial with Less Amount of Diamine Catalyst

The following approach involved the influence of different amounts of diamine and TFA, with 1, 5, 15 and 20 mol%. Based on the optimised conditions that were investigated in the previous sections, using 10 mol% of diamine and TFA, the results (Table 9) indicate that using 5 mol% or less results in a considerable decrease of conversion (83%) and enantioselectivity (90% ee). Unexpectedly, the conversion decreases to 43% at 15 mol% and increases again to 97% at 20 mol% with a concurrent increase of enantioselectivity of 99% ee. Based on the results, 20 mol% of diamine and TFA were selected for further optimisation.

Table 9: Screening of different mol% of catalyst

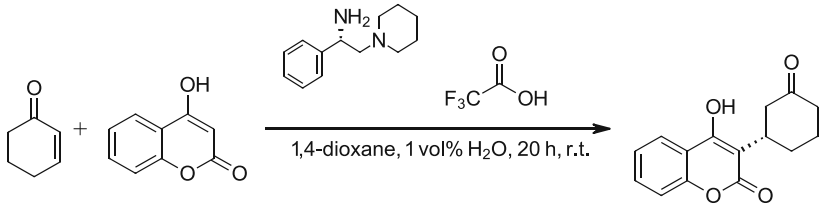

entry[a]	cat. [mol%]	conv. [%][b]	ee [%][c]	Δee[d]
1	1	83	90	0
2	5	66	90	0
3	10	91	94	-
4	15	43	94	0
5	20	97	99	5

[a]Performed with 0.16 mmol ketone, 0.17 mmol 4-hydroxcoumarin in 0.7 ml solvent at r.t. for 20 h, [b]Determined by GC-MS, [c]Determined by HPLC, [d]Δee is defined as difference between 10 mol% catalyst and x mol% catalyst

3.1.9 Solvent-Screening

The next step involved examining the relationship between conversion and enantioselectivity and various solvents, shown in Table 10. A diverse range of solvents was evaluated, including polar and nonpolar ones. In total, 12 solvents were tested, covering a broad range in terms of relative permittivity, from 2.25 F/m (1,4-dioxane) to 80.10 F/m (H_2O). It is essential to mention that no additional water was used to evaluate the impact of pure solvents without the presence of water. The results confrm that relative permittivity plays an important role in the progress of the reaction. DMF and H_2O, which have the highest relative permittivity among the solvents, lead to little (DMF, 16 %) or non-detectable (H_2O) conversion as well as non-detectable enantioselectivity. While results achieved with DMF were not very promising, methanol delivered better results with 74 % conversion and 62% ee. The best conversion was performed with solvents with a relative permittivity of 4.50 to 7.60 F m^{-1}. A plausible explanation could be that the electrostatic forces between the amine and the acidic counterpart strongly depend on the relative permittivity of the solvent. If the relative permittivity is higher, the catalyst efficiency will decrease, thus resulting in lower conversion rates. The reason is that the catalytic system cannot form the ion pair required for substrate conversion. Conversely, the conversion will decrease if the dielectric constant is too low. Yet, according to the data, there seems to be no relation between enantioselectivity and relative permittivity. Nevertheless, the best

enantioselectivities were achieved with 1,4-dioxane, THF, 2-methyl-THF, MTBE and toluene, with conversions above 80 %, except toluene (73 % conversion). Even though MTBE delivered the best results in both conversion (88 %) and enantioselectivity (92% ee), the selection of 2-methyl-THF was favoured due to its ecological aspects compared to MTBE. It enables the same enantioselectivity; even the conversion amounts to 87%.

Table 10: Solvent screening

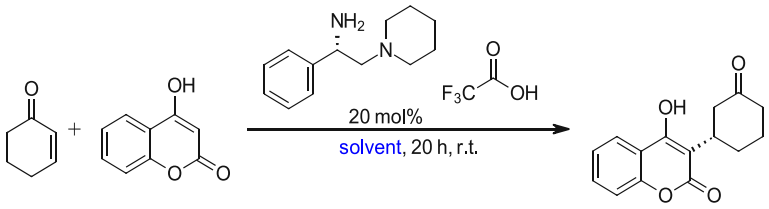

entry[a]	solvent	ε [F m^{-1}]	conv [%][b]	ee [%][c]	Δee[e]
1	1,4-Dioxane	2.25	81	92	-
2	THF	7.58	86	92	0
3	2-Methyl-THF	6.97	87	92	0
4	MTBE	4.50	88	92	0
5	DCM	8.93	64	89	0
6	1,2-Dichloroethane	10.36	69	88	0
7	Dibutylether	3.10	81	85	0
8	Toluene	2.38	73	92	0
9	Methanol	32.70	74	62	0
10	Water	80.10	n.d.[d]	n.d.	0
11	DMF	36.70	16	n.d.	0
12	Chloroform	4.81	71	90	0

[a]Performed with 0.16 mmol ketone, 0.17 mmol 4-hydroxcoumarin, 20 mol% diamine and 20 mol% acid in 0.7 ml solvent at r.t. for 20 h, [b] Determined by GC-MS, [c] Determined by HPLC, [d] n.d. = not detectible, [e]Δee is defined as difference between 1,4-dioxane and solvent

3.1.10 Substrate Screening

The approach started with the branched cyclohexenones, 3-methyl-2-cyclohexen-1-one and 4,4-dimethyl-2-cyclohexen-1-one (Table 11). The reactant was 4-hydroxycoumarin, as in the previous screenings. The parameters were the same as in section 3.1.6, where 2-methyl-THF was used instead of 1,4-dioxane. There was no conversion, hence no enantioselectivity detectable. The reason might be that the formation of the product is sterically not favourable due to the bulkiness of 4-hydroxycoumarin. The orbitals of the oxygen-atoms of 4-hydroxycoumarin overlap with the hydrogen atoms of the methyl groups, making it impossible for coumarin to be attached to the branched 2-cyclohexen-1-one. Then, the investigation continued with 2-cyclohexen-1-one and different reactants, such as pyrones, chromenes, and warfarin. Overall, excellent enantioselectivity for 4 out of 5 molecules was achieved, with 99% ee. The only implementation that did not work quite well was the conversion of 2-methylnaphthochinone with 11 % yield and no detectable enantioselectivity. The best conversion

was obtained with 4-hydroxy-6-methyl-2-pyrone, resulting in a nearly complete turnover of 98%. 58% yield was achieved with 2-hydroxy-1,4-naphthochinone, and 44% yield was attained with the synthesis of warfarin. The results suggest that the presence of a hydroxyl group on the reactant is necessary for the conversion. The catalyst also interacts with the reactant and guides it to the enone. If there is no hydroxyl group, as in 2-methyl-1,4-naphthochinone, then it will result in low conversion and very poor to no enantioselectivity.

Table 11: Results of substrate screening

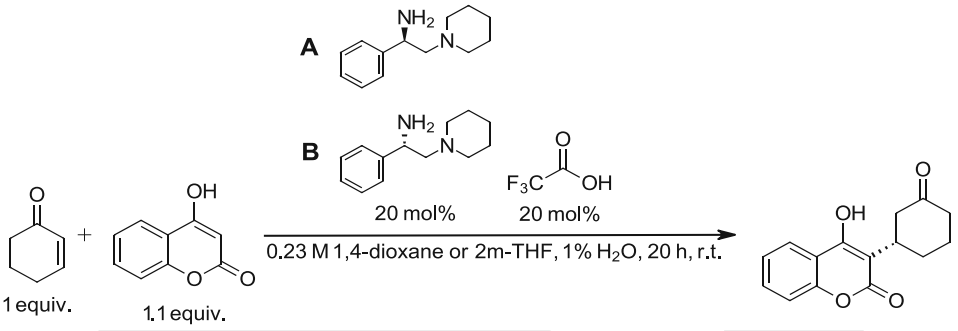

entry	product	catalyst salt	yield [%]	ee [%]
1	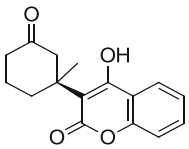 23	-	n.d.	n.d.
2	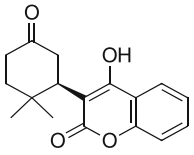 24	-	n.d.	n.d.
3	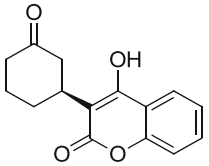 25	A (*D*) B (*L*)	89 95	99 99
4	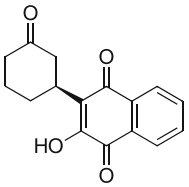 26	A B	58 45	99 99

5	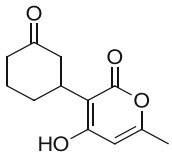 27	A B	98 84	99 99
6	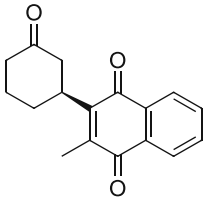 28	A B	11 8	n.d. n.d.
7	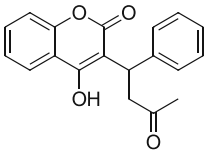 29	A B	44 59	99 99

[a]Determined by GC-MS, [b]Determined by HPLC

3.2 Synthesis of the Diamine Moiety of the Catalyst

3.2.1 Original Synthesis Path of the Diamine

The significant advantages of using the diamine as catalyst are its simple synthesis and low cost of chemicals. Except for the last step, all the other steps were performed under mild conditions (room temperature, atmospheric pressure) and in less than 24 h (**Figure 27**)—all the diamines were derived from amino acids.

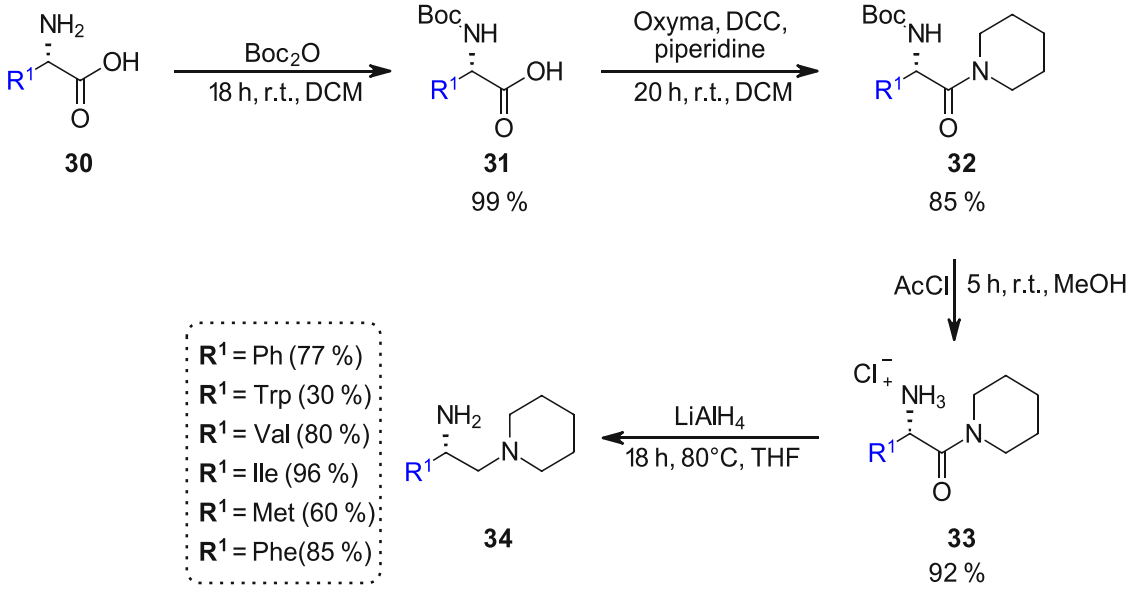

Figure 26: Synthetic pathway of the diamine. R^1 depicts the amino acid used for the synthesis. ***Ph*** *= Phenyl;* ***Trp*** *= Tryptophan;* ***Val*** *= Valine;* ***Ile*** *= Isoleucine;* ***Met*** *= Methionine;* ***Phe*** *= Phenylalanine*

Initially, the amine moiety of the amino acid was protected *via* the conventional *tert*-butoxycarbonyl (Boc) protecting group. The reaction was efficient since a 99 % yield of **31** was obtained.[84] The next step involved coupling the protected amino acid with the amine. Regardless of the amine, the same conditions were employed. Usually, a combination of dimethylaminopyridine (DMAP) and *N, N'*–dicyclohexylcarbodiimide (DCC) is used to couple acid moieties. In this type of coupling, oxyma, instead of DMAP, proved to be the better coupling agent, resulting in an 85% yield of **32**.[85] Also, the reaction conditions were mild in this case and the reaction was completed in less than 24 h. The product was purified via column chromatography. After the successful synthesis of the amide, **32** had to be deprotected for the subsequent reduction, with the help of acetyl chloride and dry methanol under standard temperature and pressure. This step was much faster than the previous, with a reaction time of 5 minutes and satisfying results of 92% yield.[85] Without further purification, the reduction of **33** was introduced as an intermediate step to synthesise **34**, using lithium aluminium hydride and dry THF, since water would destroy the $LiAlH_4$. This time, the reaction was performed under a higher temperature (80 °C) than in the previous steps.[86] All products were purified via column chromatography. Depending on the amino acid, different yields were obtained ranging from 30% (tryptophan) to 96% (isoleucin).

3.2.2 Alternative Synthesis Path of the Diamine

Meanwhile, an alternative synthetic route for the diamine was evaluated, comprising only two steps instead of four. The starting material was an amino acid (in this case, phenylglycine) as well, whose amine moiety was directly coupled to the amide,[87] protection and deprotection of the amine functionality.[85] As a coupling agent, we used piperidine and, instead of DCC and oxyma, only dimethyldipiperidinesilane[87] (**35**) was used as a "supporter". The preparation of dimethyldipiperidinesilane is depicted in Figure 28**.**

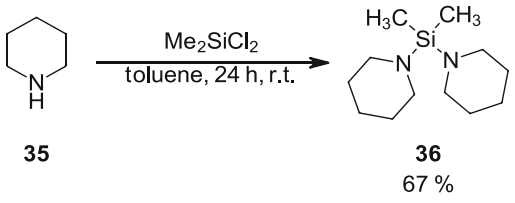

35 **36**
67 %

Figure 27: Synthesis of dimethyldipiperidinesilane[87]

After purification, 47% yield of the amide was obtained. The non-protonated amine was formed instead of the ammonium salt as in the original path.[86] The reduction step was performed under the same conditions as in the original synthetic pathway. 84% yield of the final product was obtained (Figure 29). An NMR was recorded for the confirmation of the success of the reduction; the obtained product was recovered pure, thus no further purification was necessary. Evidently, this is a

considerable advantage compared to the original synthetic path. The only question that remained was its enantioselectivity.

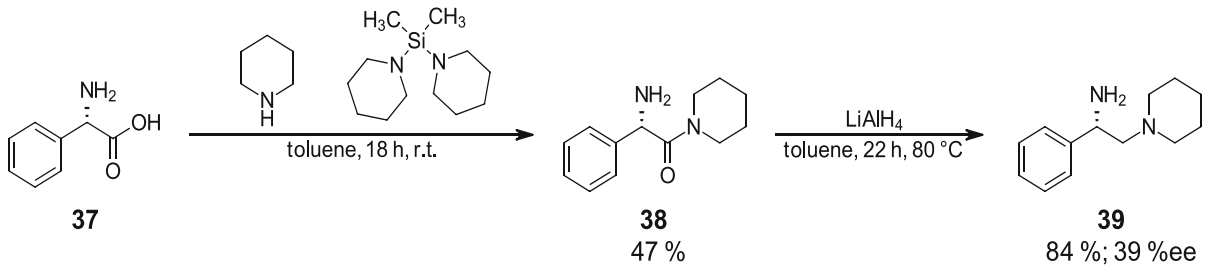

Figure 28: Alternativ synthesis of diamine

First, a reference reaction with known yield and enantioselectivity was performed for comparison, using the diamine synthesised via the original path. Even though the conversion of the product, catalysed by **39**, was comparable to the conversion of the reference reaction, the enantioselectivity was significantly lower, resulting in only 30% ee. Also, the other enantiomer was synthesised, but the enantioselectivity was not promising either. Comparison of the specific rotation of the pure (*D*)-enantiomer ($[\alpha]_D^{20}$ = –50.00 °dm^{-1} cm^3 g^{-1}) and the (*D*)-enantiomer, synthesised by the new approach ($[\alpha]_D^{20}$ = – 19.52 °dm^{-1} cm^3 g^{-1}; 39% ee), showed that the synthesised diamine was not as enantio-pure as the diamine from the original synthesis. Therefore, it was concluded that racemisation is occurring during the synthesis of the diamine, even though the enantiomer-pure amino acid was used as the staring material. Whether the racemisation takes place during the coupling or the reduction has yet to be deciphered. For further optimisation we selected the original synthetic pathway since it affords the enantiomer-pure diamine.

3.3 Synthesis of the Phosphoric Acids

The synthesis of all phosphoric acids was performed in two steps (Figure 30), Whether an eight-membered or a biphenol-derived phosphoric acid was synthesised, the first step required the coupling of the phenol-based compounds.

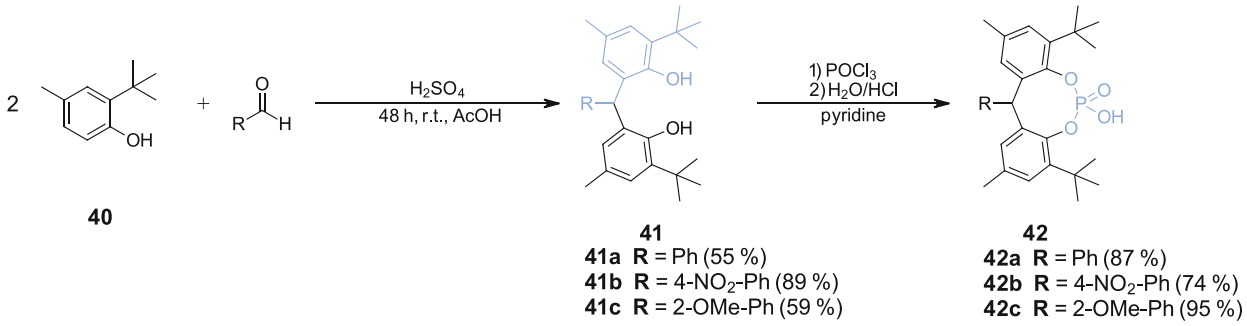

Figure 29: Synthesis of eight-ring phosphoric acids

In the case of the eight-membered phosphoric acid, the coupling of two phenol-type molecules, with an aldehyde as the connecting unit, was performed under acidic conditions. Depending on the residue

on the aldehyde, yields from 55% (**R** = Ph) to 89% (**R** = 4-NO_2-Ph) were obtained. The intermediate **41** was then converted into phosphoric acid using phosphoryl chloride ($POCl_3$), followed by hydrolysis with aqueous hydrochloric acid. The obtained yields ranged from 74% (4-NO_2-Ph) to 95% (**R** = 2-OMe-Ph).

In the case of the biphenol-derived phosphoric acid (Figure 31), the coupling of the phenol-derivatives was performed with bis-(*tert*-butoxy) oxide in chlorobenzene, resulting with 76 % yield of **44**. The synthesis of the phosphoric acid from the intermediate was performed under the same conditions as the eight-membered phosphoric acid.

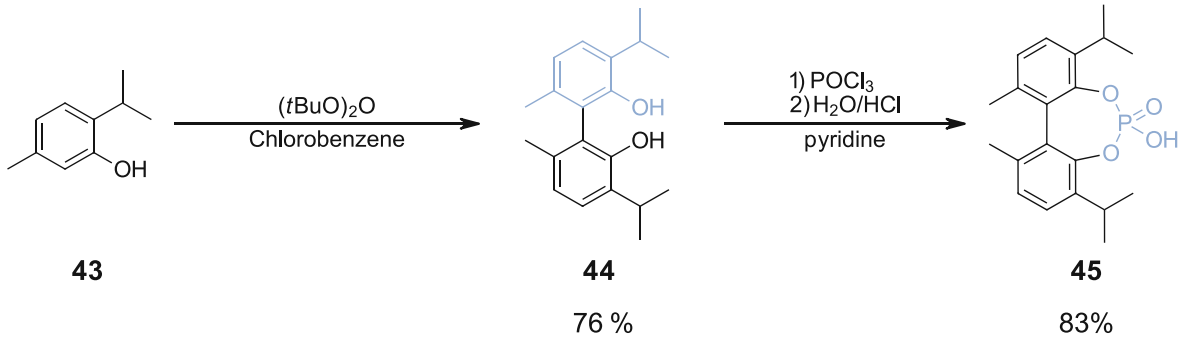

43 **44** **45**

76 % 83%

Figure 30: Synthesis of the diphenyl-based phosphoric acid

3.4 Immobilisation of the Catalyst

Considering the remarkable results obtained during the batch reactions, the possibility of immobilising the catalytic system was investigated. Three different immobilisation options were evaluated. One was the chemisorption of the diamine on a supporting material, such as silica. However, it required the modification of the diamine to enable the attachment on the solid support. The other two approaches are based on physisorption. One was the adsorption on a tungsten-based polyoxometalate support, and the other approach was an ionic liquid-accompanied immobilisation on a silica-support. Of course, chemisorption would be beneficial due to the low possibility of catalyst leaching compared to physisorption. However, chemisorption accompanied by a trade-off in catalytic activity. Nevertheless, the goal was to evaluate the feasibility of a continuous conversion *via* flow chemistry. The (*D*)-enantiomer of diamine **1** was used for all three immobilisation approaches.

3.4.1 Chemisorption

The synthesis followed the approach of Wechakorn *et al.*, but instead of using silica-coated Fe_3O_4–nanoparticles (Fe_3O_4 @SiO_2),[88] pure silica was used instead. Wechakorn attached their catalyst *via* click reaction. The final support contained an alkyne moiety on the catalyst and an azide group attached on the solid material. In the approach with pure silica, the biggest obstacle was the feasibility

of the immobilisation of our catalyst *via* chemisorption. To afford the chemical bonding of the catalyst on the solid support, the silica surface had to be modified by attaching an azide moiety. Also, the diamine was not suited for immobilisation with its current chemical structure. The idea was to start with (*D*)-4-hydroxyphenylglycine instead of the phenylglycine (Figure 33).

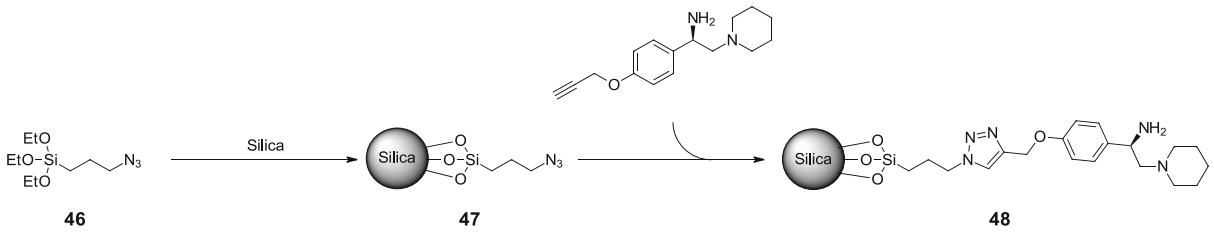

Figure 31: Synthetic pathway of the immobilisation of the modified diamine

The first step was, as well as in section 3.2.1, protection of the amine group, which resulted in an excellent yield of over 99%. Consequently, the next step was coupling of the acid group to piperidine under analogous conditions, as in section 3.2.1, which led to 59% yield after purification via liquid chromatography. The next step was the introduction of propargyl bromide to the hydroxy group of the benzene ring, which afforded 96% yield without purification.[89] The two subsequent steps were identical to the synthesis of the original diamine **34**, except that the reduction was performed for 48 h instead of 18 h. The deprotection worked excellently with over 99% crude product, yet after reduction and following purification, only 26% of the final product **54** was obtained. This is much less than the yield of the phenylglycine derived diamine (77%). Another approach with (*L*)-4-hydroxyphenylglycine was performed, to investigate whether the low yield could be attributed to an experimental error, resulting in a 14% yield of the diamine. An explanation for the low yield might be that the attachment of propargyl bromide did not work as efficiently as expected. A purification step can be inserted in the 3rd and 4th steps to understand better the significant loss in the efficiency of this reaction.

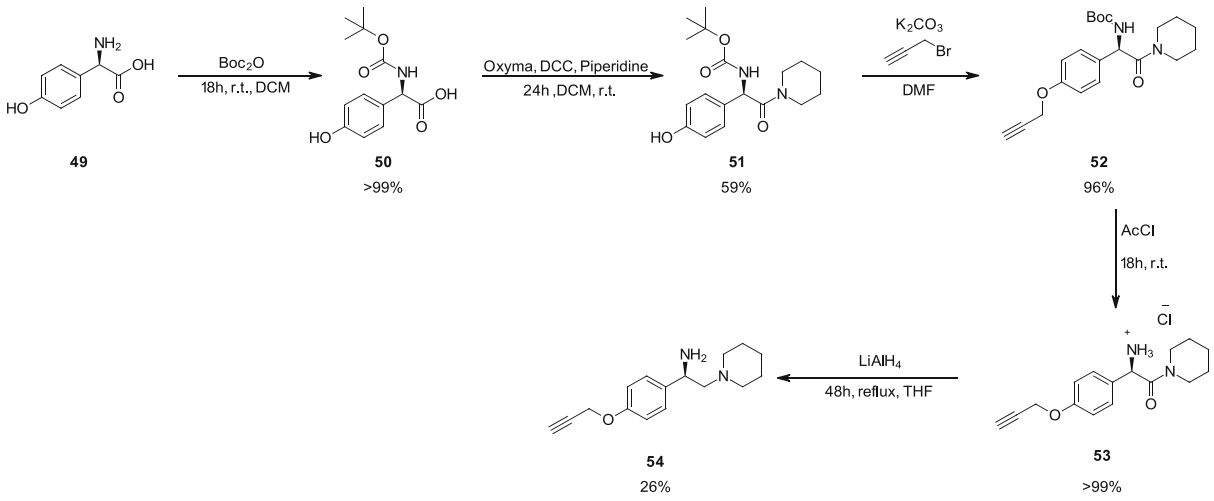

Figure 32: Scheme of the synthesis of the modified diamine for the subsequent click-reaction

To attach the modified diamine on the support, the supporting material also needed to be modified. Pure silica was used since, unlike Wechakorn *et al.*, we only wanted to investigate the possibility of immobilising catalyst **54** without any functionalisation of nanoparticles. Fe_3O_4 @SiO_2 and silica have the conventional silica surface, which is mandatory for the click reaction. Another massive advantage of silica is that it is commercially available, and no additional coating steps are required, as shown in the work of Wechakorn *et al*. Initially, the azide was attached onto the silica surface. First, the chloride moiety in (3-chloropropyl) triethoxysilanewas substituted by an azide by addition of sodium azide (NaN_3).[89] This reaction was simple, clean, and fast, resulting in 67% yield (Figure 34).

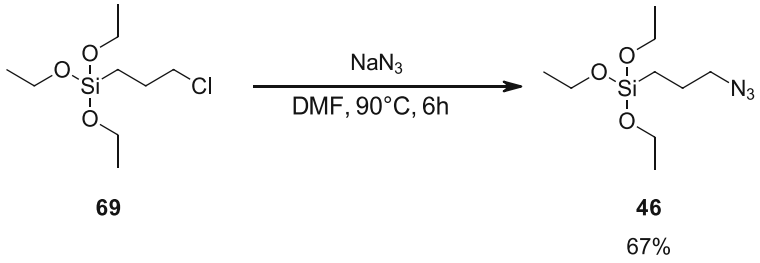

Figure 33: Substitution of the chloride moiety by an azide moiety

Subsequently, the intermediate **46** was attached to the silica surface under standard temperature and pressure. Subsequently, the click reaction was performed. A trial reaction was performed for a simple and fast determination of the success of the diamine chemisorption; Michael-addition of 2-cyclohexen-1-one and 4-hydroxycoumarin. The conversion was 31%. Compared to that, a reference reaction, without the presence of the catalyst, was performed, resulting with non-detectable yield. which proved the success of the immobilisation of the catalyst.

3.4.2 Ionic liquid supported physisorption

Another immobilisation approach was the physisorption of the catalyst on silica, supported by an ionic liquid (Figure 35), based on an approach by Hagiwara *et al.*, where MacMillan catalysts were used. According to Hagiwara and co-workers, the catalytic activity and enantioselectivity slightly depend on the ionic liquid.[90]

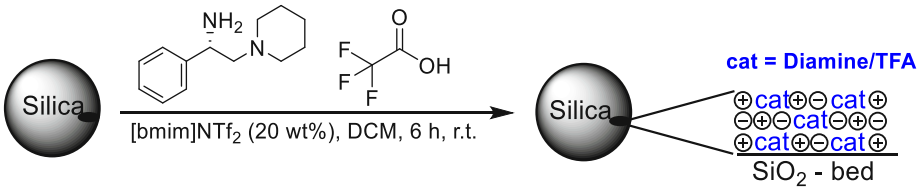

Figure 34: Scheme of the ionic liquid supported immobilisation of diamine/TFA

This developed procedure is straightforward, containing only silica, our catalytic system, and an ionic liquid. The ingredients are simply mixed and stirred for a specific time. After filtration and drying, a colourless solid is obtained which is ready for further use. Contrary to the chemisorption and the

physisorption of the catalyst on polyoxotungstate,[94] the catalytic salt of diamine and the acid had to be formed prior to immobilisation. We decided to use the ionic liquid $[C_4mim]NTf_2$ (Figure 36) because it exhibited the best performance in the work of Hagiwara *et al*.[89]

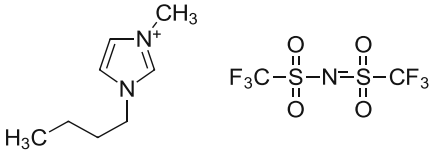

Figure 35: Structure of ionic liquid $[C_4mim]NTf_2$

Following immobilisation, the weight of the silica powder increased, by 495 mg, which implied that the ionic liquid and the catalytic system had been loaded onto the silica. To prove the success of the immobilisation, a trial with 4-hydroxy-6-methyl-2-pyrone and 2-cyclohexen-1-one was performed with a remarkable conversion of 93% and 96% ee, which demonstrated the successful immobilisation of the catalytic system.

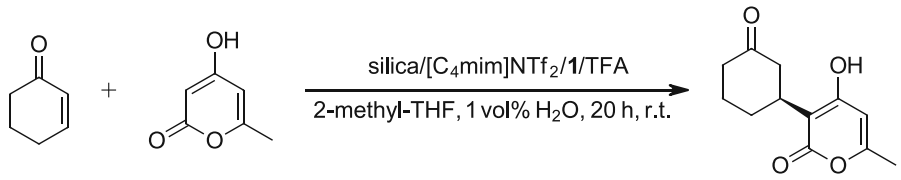

Figure 36: Overview of the reference reaction and its conditions used for the trial of the immobilised catalyst

An issue that occurred was the consistency of the product. Under homogeneous catalysis a white solid remained. However, the consistency of the remaining product in this experiment was quite pasty. For that reason, a ^{19}F-NMR was performed to verify if this observation could be attributed to catalyst leaching off the solid support during the reaction. TFA and $[C_4mim]NTf_2$ contain a fluorine atom at different shifts, as opposed to the product. According to the recorded spectrum, leaching indeed occurred, which is detectable as 2 signals at 79.859 ppm ($[C_4mim]NTf_2$) and 75.728 ppm (TFA). Nevertheless, further research was continued with the exhibition of the reaction in continuous mode, since at this stage a proof-of-concept flow reaction rather than a fine-tuned system was aimed. A presumption to solve the leaching issue would be the utilisation of a different solvent, with comparable enantioselectivity and conversion to 2-methyl-THF, but with a less relative permittivity. The results showed that solvents with a dielectric constant of approximately 7 F m^{-1} and higher result in leaching. Two candidates showed comparable enantioselectivity (see Table 8) with 2-methyl-THF (92 %ee), yet a lower dielectric constant. The best candidates would be 1,4-dioxane (ε = 2.25 F m^{-1}; 81% conv.; 92 %ee) and toluene (ε = 2.38 F m^{-1}; 73% conv.; 92 %ee).

3.4.3 Polyoxometalate Supported Physisorption

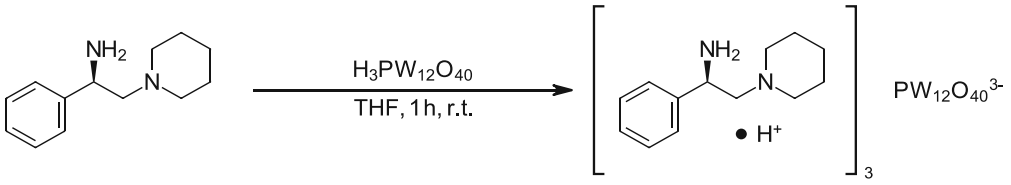

Figure 37: Scheme of the immobilisation of the diamine on polyoxotungstate

Another approach was to immobilise the catalyst on polyoxotungstate, based on the work of Luo S. *et al.*, who immobilised chiral amines on polyoxometalates.[93] Also, here, the preparation of the immobilised catalyst was quite simple and fast. Another advantage is that no further modification of the diamine was necessary. In this approach, only the diamine had to be attached to the polyoxotungstate. This meant that the catalytic system with diamine and TFA had to be formed *in situ* during the reaction. The success of the immobilisation was confirmed by trial with 4-hydroxy-6-methyl-2-pyrone and 2-cyclohexen-1-one (same reaction as in Figure 37, just with polyoxometalate) to compare the results with the ionic liquid supported approach. Even though the conversion decreased to 71%, excellent enantioselectivity of 99% ee was achieved. Additionally, no leaching occurred using 2-methyl-THF as the solvent.

3.5 Preparation for Continuous Flow – Kinetic Studies

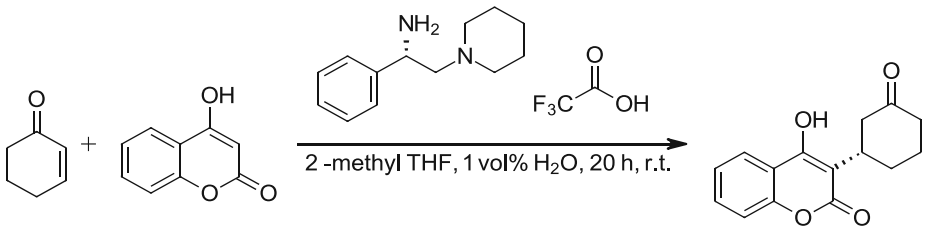

Figure 38: Reaction used for kinetic studies

Before the procedure for the continuous-flow approach, the temporal progress of the reaction had to be investigated to adjust the flow rate in the continuous mode. The progress of the reaction was monitored for 5 hours. According to the collected data (see Figure 40), a conversion of 83% was reached after 4 h and after 5 h, 86% of the 2-cyclohexen-1-one was converted. This implies that after 4 h, the curve starts to flatten sharply.

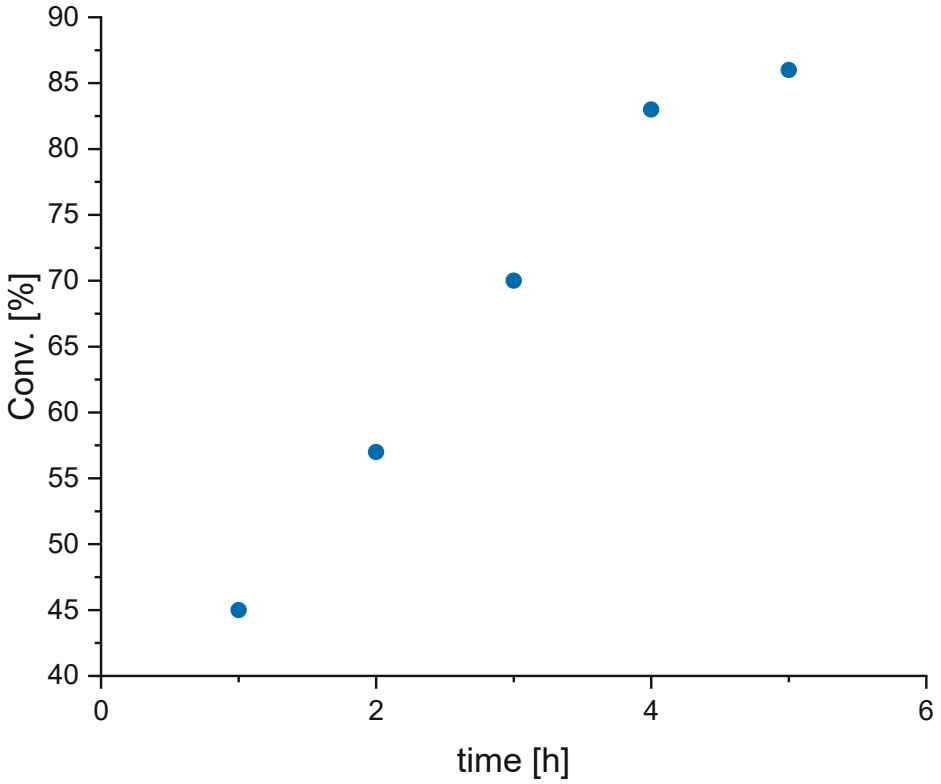

Figure 39: Temporal progress of the Michael-addition of 2-cyclohexen-1-one and 3-hydroxy-6-methyl-2-pyrone

A trial without catalyst was also performed, whereby a conversion below 1% was achieved; therefore, the necessity of the catalyst in this reaction was demonstrated.

3.6 Continuous Flow Reaction – First Trials

3.6.1 Trial with Ionic Liquid Supported, Immobilised Catalyst

The physisorbed catalysts were selected for the continuous-flow reaction experiments, since they exhibited superior performance than the chemisorbed catalyst. Moreover, the chemisorption process still requires optimisation and further improvement before it can be applied. We started with the ionic liquid immobilised, using a flow rate of 56.0 µl min^{-1}, under room temperature. Taking into consideration the previously optimised conditions, 2-cyclohexen-1-one was used as the substrate and 4-hydroxycoumarin as the reactant. Additionally the conversion and stability of the catalyst on the solid support was determined. A conversion of 5% was achieved, which confirmed the feasibility of the catalytic system to function in continuous-flow mode. However, a significant disadvantage, namely leaching, also occurred in this trial. To increase the conversion, the dwell time of the reaction mixture (substrate and reactant) was increased by decreasing the flow rate to 25.4 µl min^{-1}, but no significant change in conversion was detected. The easiest way to determine possible leaching was to record a

^{19}F-NMR since TFA and NTf_2^- contain fluorine atoms. Leaching was verified based on the two peaks that were observed in the ^{19}F-NMR spectrum; one peak was corresponding to TFA at 75.7 ppm, and the other was for NTf_2^- at 78.9 ppm. With the catalyst components being "washed out" of the silica, less diamine/TFA was present on the solid support. Before introducing the reaction mixture into the immobilised catalytic system, the silica was moistened with the solvent. The results of the screening of the catalytic system (section 3.1.9) depict the importance of the substrate/catalyst ratio. Less catalyst results with less conversion; this discovery also verifies this case. The leaching issue must be addressed to maintain the loaded amount of catalyst immobilised on silica.

3.6.2 Trials with Polyoxometalate Immobilised Catalyst

The following approach was the trial with the tungsten-based polyoxometalate immobilised catalyst. Previous investigations showed that no leaching occurred in this approach. According to the section above, the conversion should be higher than in the silica-supported approach due to the lack of leaching, using the same flow rate. Therefore, we decided to use the same flow rate (25.4 µl min^{-1}) for this approach to compare the results between the silica-supported catalytic system and the polyoxotungstate-supported approach. The procedure slightly differs from the one above (section 3.6.1) since only the diamine is immobilised on the polytungstate, while the catalytic system, including TFA, had to be formed in situ. The results showed a conversion of 4.5%. Even though one might expect the conversion to be higher than in the ionic liquid-supported approach, the conversion was even lower than in the entry above, with 56.0 µl min^{-1}. A possible explanation could be that the flow rate in the polyoxotungstate-supported approach was too high. Ideally, further optimisation with lower flow rates should be performed.

4 Conclusion

In conclusion, the promising potential of an amino acid derived diamine-catalyst for the Michael addition of cyclic enones and Michael donors, in combination with an acidic counterpart was proved. The optimal catalytic system was the combination of a phenylglycine derived diamine and TFA as the acidic part. Additionally, the importance of an acid, for the enantioselectivity was proved. Subsequently, screening of various amounts of catalyst and water were performed. Further research of different solvents with low to high dielectric constants exhibited that 2-methyl THF was the best candidate for the synthesis of warfarin and its analogues. Further investigation of different substrates with 2-cyclohexenone gave yields, ranging from 44% (warfarin) to 98% (4-hydroxy-6-methyl-2-pyrone). Yet the impossibility of 3-substitued cyclohexenones was demonstrated.

In the second part of the thesis, successful immobilisation of the catalyst on silica (supported by ionic liquids) and polyoxotungstate *via* physisorption and on silica *via* chemisorption. For the chemisorption a modified phenylglycine derived diamine was attached to a modified silica support *via* click-chemistry. Batch reactions, using the immobilised catalyst, exhibited its potential for reactions in continuous mode for the physisorbed catalyst, yet no results were achieved with the chemisorbed catalyst. First approaches for continuous-flow reactions were performed with the catalyst immobilised on silica and polyoxotungstate. But leaching occurred at the catalyst, physisorbed together with $[C_4mim]NTf_2$ on silica.

5 Experimental

5.1 Materials and Methods

All purchased chemicals from commercial suppliers were used without further purification, unless otherwise stated. Dry solvents were pre-distilled and desiccated on aluminium oxide (PURESOLV, Innovative Technology). Column chromatography was performed on standard manual glass columns using Merck (40-60 µm) silica gel with pre-distilled solvents (PE: light petrol, EtOAc: ethyl acetate, Et_2O: diethyl ether). Precoated aluminium-backed plates were purchased from Merck (silica gel 60 F254) for TLC analysis. UV active compounds were detected at 254 nm. Non-UV active compounds were detected using a vanillin staining solution (5% H_2SO_4 and vanillin in ethanol). Microwave reactions were performed on a Biotage Initiator Classic in 20ml pressure-tight glass vials.

^{1}H,^{13}C, and ^{19}F NMR spectra were recorded on a Bruker Avance UltraShield 200 MHz or 400 MHz spectrometer and chemical shifts were reported in ppm using TMS (tetramethylsilane) as an internal standard. Coupling constants (J) are given in Hz. For NMR purposes, the following abbreviations are used: s (singlet), d (doublet), t (triplet), q (quartet), m (multiplet), brs (broad singlet), dd (doublet of doublets), ddd (doublet of doublets of doublets), td (triplet of doublets), dt (doublet of triplets).

GC yields were determined using a BGB5 column and an FID detector. Chiral GC measurements were performed on chiral BGB columns (BGB 173, BGB 175) using an FID detector to determine enantiomeric excess. Optical rotation was measured on an Anton Paar MCP500 polarimeter to determine the absolute configuration at the specific conditions, and the results were compared to literature values. Concentrations are given in g / 100ml.

Phosphoric acids were synthesised and provided by Dipl.-Ing. Fabian Scharinger.

5.2 Synthesis of Diamine Catalyst *via* an Alternative Route

5.2.1 Dimethyldipiperidinosilane

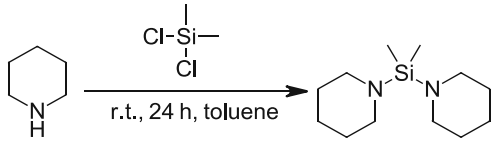

35 **36**

In a round-bottom flask, piperidine (15.824 g, 0.186 mol, 4.0 eq.) was dissolved in toluene (48 ml) and cooled to 0°C. Dichlorobis(methyl)silane (5.992 g, 0.046 mol, 1.0 eq.) was added dropwise. A dense solid was formed. More toluene (15 ml) was added, and the suspension was stirred for 24 h at room temperature. Subsequently, the mixture was filtered over celite and washed with toluene. Removal of the solvent gave a slightly yellow liquid (7.041 g, 67%). The product was used without further purification.

5.2.2 (*S*)-2-Amino-2-phenyl-1-piperidino-1-ethanone

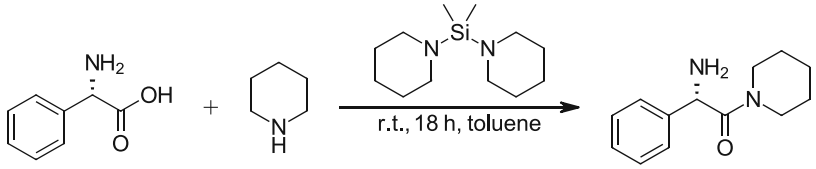

37 **35** **38**

In a round-bottom flask, (*L*)-phenylglycine (2.497 g, 0.017 mol, 1.0 eq.) was dispersed in toluene (15 ml). Piperidine (5.626 g, 0.066 mol, 4.0 eq.) was added, followed by the slow addition of dimethyldipiperidinosilane (8.453 g, 0.037 mol, 2.3 eq.). The mixture was stirred for 18 h at room temperature. After 18 h, the solution was cooled down to 0 °C. A saturated solution of ammonium carbonate was added slowly until the turbid solution cleared. Afterwards, EtOAc was added. The phases were separated, and the aqueous phase was extracted three times with EtOAc. The combined organic phases were dried over anhydrous sodium sulphate. Removal of the solvent gave an orange, viscous liquid. The crude product was purified *via* column chromatography (5% MeOH: DCM, R_f = 0.29, visualisation *via* ninhydrin-staining). The pure product (1.708g, 47%) was obtained as an orange viscous liquid.

^{1}H NMR (400 MHz, $CDCl_3$) δ7.26 – 7.20 (m, 5H, *H*-arom), 4.68 (s, 1H, *CH*-NH_2), 3.63 (ddd, 3H, CH_2-N -CH_2), 3.38 (ddd, 1H, CH_2-N -CH_2), 3.15 (m, 2H), 2.3 (s, 2H, -NH_2), 1.45 – 0.89 (m, 6H, CH_2-CH_2-CH_2 piperidine)

Analytical data was in accordance with literature.[92,93]

5.3 Synthesis of Diamine Catalyst *via* Original Route

5.3.1 (*S*)-1-Phenyl-2-piperidinoethylamine

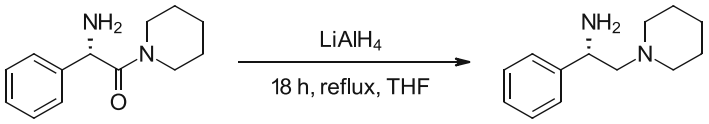

38 **39**

A solution of (*S*)-2-amino-2-phenyl-1-piperidino-1-ethanone (1.708 g, 0.008 mol, 1.0 eq.) in anhydrous THF (55 ml) was placed in a three-neck round-bottom flask, and cooled down to 0 °C. Then $LiAlH_4$ (1.188 g, 0.031 mol, 5.0 eq.) was added portion-wise to the solution. Subsequently, the solution was stirred at room temperature for 15 minutes, heated to 80 °C and stirred for 22 h. After cooling down to 0 °C, distilled water (4 ml) was added carefully (vigorous foaming), followed by a solution of NaOH (15%, 8 ml) and it was kept stirring for another 10 minutes. Anhydrous Na_2SO_4 was added to remove water. Next, EtOAc (20 ml) was added. The solid was filtered off *via* celite, and the solid was washed several times with EtOAc. The organic phase was extracted twice with 1 M NaOH and once with brine. After drying over Na_2SO_4, the solvent was removed, giving an orange oily liquid (1.338 g, 84%).

^{1}H NMR (400 MHz, $CDCl_3$) δ7.32 – 7.14 (m, 5H, *H*-arom), 4.0 (s, 1H, *CH*-NH_2), 2.49 (s, 2H, -*NH_2*), 2.39 – 2.17 (m,4H, *CH_2*-N -*CH_2*), 1.91 (s, 2H, *CH_2*-CH), 1.60 – 1.38 (m, 4H, *CH_2*-CH_2-*CH_2*), 1.36 (dd, 2H, CH_2-*CH_2*-CH_2)

Analytical data was in accordance with literature.[94]

5.3.2 Ethyl (2Z)-2-cyano-2-(hydroxyimino)acetate (oxyma)

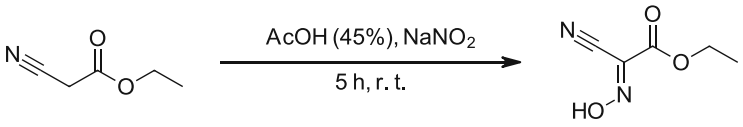

55 **56**

Ethyl cyanoacetate (7.55 ml, 0.071 mol, 1.0 eq.) in aqueous acetic acid (45%, 32 ml) was stirred at 0°C for 15 minutes. Afterwards, sodium nitrite (14.637 g, 0.22 mol, 3.0 eq.) was added portion-wise to the mixture. A yellow solid formed quickly. The mixture was stirred for 18 h at room temperature. Subsequently, diethyl ether (50 ml) was added. Water was added until the solid completely dissolved. The organic phase was separated, and the aqueous phase was extracted two times with diethyl ether. The combined organic phases were washed two times with water and once with brine. The organic phase was dried over anhydrous sodium sulphate. A yellow solid (9.283 g, 92%) was obtained after removing the solvent and drying at a high vacuum (0.1 mbar).

^{1}H NMR (400 MHz, $CDCl_3$) δ4.45 (q, 2H, -*CH_2*), 1.41 (s, 3H, -*CH_3*)

5.3.3 (*S*)-(*tert*-Butoxycarbonylamino) phenylacetic acid

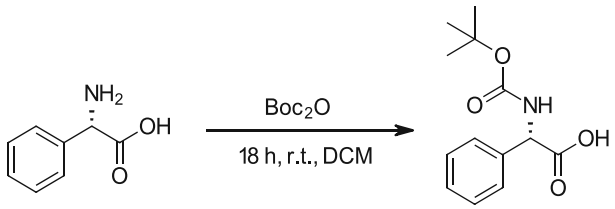

57 **58**

In a round bottom flask (250 ml), (*L*)- phenylglycine (5.000 g, 0.033 mol, 1.0 eq.) was dissolved in a mixture of THF (39 ml) and an aqueous solution of 1 M NaOH (40 ml). Afterwards, di-*tert*-butylcarbonate (8.662 g, 0.040 mol, 1.2 eq.) was added at room temperature. Shortly after the addition of Boc_2O, a white, dense solid formed, which dissolved after approx. 30 minutes. The reaction mixture was stirred for 18 h at room temperature. Subsequently, THF was removed, DCM (25ml) was added to the aqueous solution, and the biphasic solution was acidified to pH 2 with 1 M HCl. The aqueous phase was extracted three times with DCM, and the organic phases were combined and dried over anhydrous sodium sulphate. Removal of DCM gave a white, solid product (8.278 g, 99%).

^{1}H NMR (400 MHz, $CDCl_3$) δ7.51 (s,1H, -*COOH*), 7.43 – 7.29 (m, 5H, *H*-arom), 5.13 (d, *J* = 8.1 Hz, 1H, *NH*-CH), 1.40 (s, 9H, *CH_3*-Boc)

Analytical data was in accordance with literature.[95]

5.3.4 (*S*)-2-Oxo-1-phenyl-2-piperidinoethylamino-*tert*-butylformylate

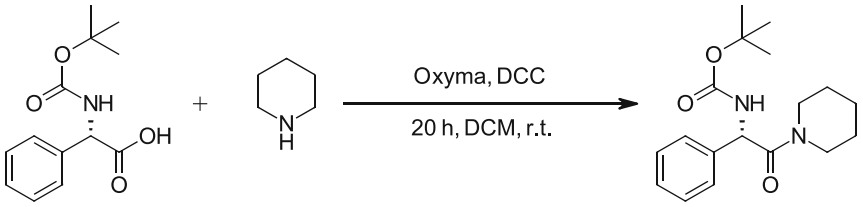

58 **35** **59**

(*S*)-(*tert)*-Butoxycarbonylamino) phenylacetic acid (5.450 g, 0.022 mol, 1.0 eq.) was dissolved in dry DCM (75 ml). Then, DCC (8.950 g, 0.043 mol, 2.0 eq.), oxyma (3.390 g, 0.024 mol, 1.1 eq.) and piperidine (4.617 g, 0.054 mol, 2.5 equiv.) were added, at 0 °C. The turbid, orange solution was stirred for 15 minutes at 0 °C. After reaching ambient temperature, the reaction mixture was stirred for 48h at room temperature. After 48h hours, cold EtOAc (50 ml) was added and the mixture was stirred for 10 minutes. The solid formed was filtered off, and the clear solution was concentrated in vacuum (20 mbar). EtOAc (25 ml) and 1 M HCl (50 ml) were added to the remaining orange liquid. DCU formed and was filtered off. Subsequently, the organic phase was extracted two times with 1 M HCl, followed by 1M NaOH (3 times) and brine. The aqueous, basic phase was extracted one time with EtOAc. The combined organic phase was dried over sodium sulphate. Removal of the solvent gave an orange, oily liquid. The product was purified *via* column chromatography (30% EtOAc: PE, R_f = 0.54, visualisation *via* ninhydrin-staining). After removing the solvent, a colourless solid (4.982 g, 75%) remained.

^{1}H NMR (400 MHz, $CDCl_3$) δ7.41 – 7.24 (m, 5H, *H*-arom), 6.12 (d, *J* = 7.6 Hz, 1H, *NH*), 5.55 (d, *J* = 7.7 Hz, 1H, *CH*-NH), 3.78 – 3.67 (m, 1H, CH_2-N), 3.47 – 3.37 (m, 1H, CH_2-N), 3.34 – 3.21 (m, 2H, CH_2-N), 1.59 – 1.47 (m, 3H, CH_2-CH_2-CH_2), 1.40 (s, 12H, CH_3-Boc + CH_2-CH_2-CH_2)

Analytical data was in accordance with literature.[96]

5.3.5 (*S*)-2-Oxo-1-phenyl-2-piperidino-1-ethanammoniumchloride

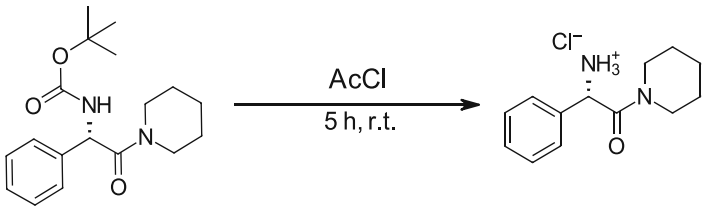

59 **60**

In a round-bottom flask, (*S*)-2-oxo-1-phenyl-2-piperidinoethylamino-*tert*-butylformylate (4.982 g, 0.016 mol, 1.0 eq.) was dissolved in dry methanol (39 ml) followed by the addition of acetyl chloride

(9.827 g, 0.125 mol, 8.0 eq.) at 0 °C. The mixture was stirred for 15 minutes. After removing the ice/water bath, the reaction was stirred for 5 hours at room temperature. The solvent was removed under vacuum, and a green solid (9.248 g, 99%) remained. The product was used for further synthesis without purification.

5.3.6 (*R*)-1-Phenyl-2-piperidinoethylamine

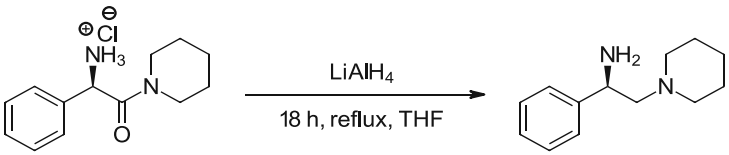

61 **62**

A solution of (*R*)-2-oxo-1-phenyl-2-piperidino-1-ethanammoniumchloride (5.222 g, 0.020 mol, 1.0 eq.) in dry THF (144 ml) was cooled to 0 °C. Then $LiAlH_4$ (3.889 g, 0.102 mol, 5.0 eq.) was added portion-wise to the solution. Subsequently, the solution was stirred at room temperature for 15 minutes and heated to 80 °C for 48 h. After cooling down to 0 °C, distilled water (4 ml) was added carefully (vigorous foaming), followed by a solution of NaOH (15%, 8 ml) and it was kept stirring for another 10 minutes. Anhydrous Na_2SO_4 was added to remove water. Next, EtOAc (20ml) was added. The solid was filtered off *via* celite, and the solid was washed several times with EtOAc. The organic phase was extracted twice with 1 M NaOH and once with brine. After drying over Na_2SO_4, the solvent was removed, giving an orange oily solution and a few solid crystals (4.121 g, 98%). The crude product was purified *via* column chromatography (30% EtOAc/PE/0.8% Et_3N). After removing the solvent, a yellow, oily liquid (2.751 g, 66%) was obtained.

^{1}H NMR (400 MHz, $CDCl_3$) δ7.35 – 7.01 (m, 5H, *H*-arom), 4.05 (dd, 1H, *CH*-NH_2), 2.51 (s, 2H, -*NH_2*), 2.38 – 2.20 (m, 4H, *CH_2*-N-*CH_2*), 2.08 (s, 2H, *CH_2*-N), 1.61 – 1.43 (m, 4H, *CH_2*-CH_2-*CH_2*), 1.41 – 1.30 (q, 2H, CH_2-*CH_2*-CH_2)

Analytical data was in accordance with literature.[94]

5.4 Synthesis of the Modified Diamine for Chemisorption

5.4.1 (*R*)-(*tert*-Butoxycarbonylamino)(*p*-hydroxyphenyl)acetic acid

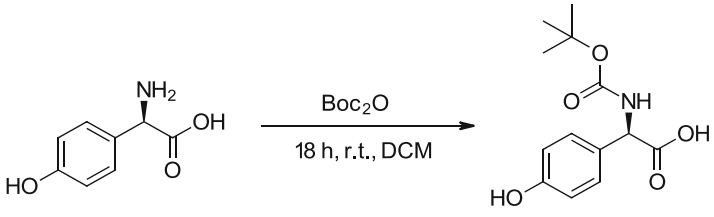

49 **50**

Prepared according to the procedure in section 5.3.3, from (*R*)-amino(*p*-hydroxyphenyl)acetic acid (3.000 g, 0.018 mol, 1.0 eq.), bis(2-methyl-2-propanyl) dicarbonate (4.700 g, 0.022 mol, 1.2 eq.), THF (21 ml) and 1 M NaOH (22 ml). Stirring for 18h at room temperature gave a white solid (5.278 g, 99%). The product was used for further synthesis without purification.

^{1}H NMR (400 MHz, $CDCl_3$) δ7.19 (s, 1H, *COOH*), 7.08 (t, 2H, *H*-arom), 6.63 (d, *J* = 8.2 Hz, 2H, *H*-arom), 3.69 (m, 1H, *OH*-arom), 1.82 – 1.76 (m, 1H, *NH*), 1.33 (s, 4H, CH_3-Boc), 1.25 – 1.16 (m, 6H, CH_3-Boc + *CH*-N)

Analytical data was in accordance with literature.[95]

5.4.2 (*R*)-1-(*p*-Hydroxyphenyl)-2-oxo-2-piperidinoethylamino-*tert*-butylformylate

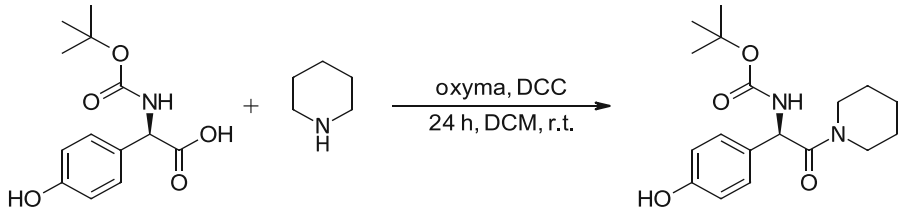

50 **35** **51**

Prepared according to the procedure in section 5.3.4, from (*R*)-(*tert*-butoxycarbonylamino)(*p*-hydroxyphenyl)acetic acid (4.797 g, 0.018 mol. 1 eq.), DCC (7.406 g, 0.036 mol, 2.0 eq.), oxyma (2.806 g, 0.020 mol, 1.1 eq.), piperidine (3.821 g, 0.045 mol, 2.5 eq.) and dry DCM (90 ml). The reaction was carried out at room temperature for 24 hours. Column chromatography (40% EtOAc: PE, R_f = 0.54, visualisation via ninhydrin-staining) gave a white, solid product (3.537 g, 59%).

^{1}H NMR (400 MHz, $CDCl_3$) δ7.132 (d, *J* = 8.6 Hz, 2H, *H*-arom), 6.65 (d, *J* = 8.6 Hz, 2H, *H*-arom), 5.42 (d, *J* = 7.7, 1H, *HO*-Ph), 3.72 – 3.61 (m, 1H, *NH*-C), 3.39 – 3.27 (m, 1H, *CH*-N), 1.56 – 1.14 (m, 19H, CH_3-Boc + CH_2-Pip)

Analytical data was in accordance with literature.[96]

5.4.3 (R)-2-Oxo-2-piperidino-1-[p-(2-propynyloxy)phenyl]ethylamino-tert-butylformylate

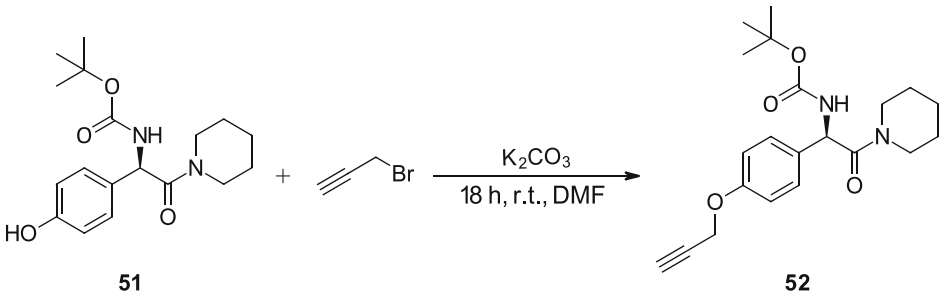

51 52

In a round-bottom flask, (*R*)-1-(*p*-hydroxyphenyl)-2-oxo-2-piperidinoethylamino-*tert*-butylformylate (2.800 g, 0.008 mol, 1.0 eq.) was dissolved in dry DMF (16 ml) and flushed with argon. After the addition of potassium carbonate (3.474 g, 0.25 mol, 3.0 eq.), the mixture was cooled with an ice/salt bath. Then 3-bromopropyne (80% in toluene, 1.400 g, 0.011 mol, 1.3 eq.) was added slowly to the solution. The solution was allowed to reach room temperature and, then, stirred for 18 h. Afterwards, DMF was removed in vacuum (20 mbar), and a saturated solution of ammonium chloride (200 ml) was added and the mixture was stirred for 2 hours. Then, EtOAc (30 ml) was added and the mixture was stirred for 30 minutes. The two phases were separated, and the aqueous phase was extracted twice with EtOAc. Again, a saturated solution of NH_4Cl (200 ml) was added to the combined organic phases and stirred for another 1.5 h. Subsequently, the phases were separated, the organic phase was dried with anhydrous Na_2SO_4, and the solvent was removed to give a brown, very viscous liquid (2.987 g, 96%). The product was used for further synthesis without purification.

^{1}H NMR (400 MHz, $CDCl_3$) δ7.24 (d, *J* = 8.7 Hz, 2H, *H*-arom), 6.85 (d, *J* = 8.7 Hz, 2H, *H*-arom), 6.03 (d, *J* = 7.6 Hz, 1H, *NH*), 5.45 (d, *J* = 7.6 Hz, 1H, *CH*-N), 4.60 (d, *J* = 2.4 Hz, 2H, CH_2-PhO), 2.45 (s, 1H, *H*C≡C), 1.53 – 1.24 (m, 19H, CH_3-Boc + CH_2-Pip)

Analytical data was in accordance with literature.[96]

5.4.4 (*R*)-2-Oxo-2-piperidino-1-[*p*-(2-propynyloxy)phenyl]-1-ethanammonium chloride

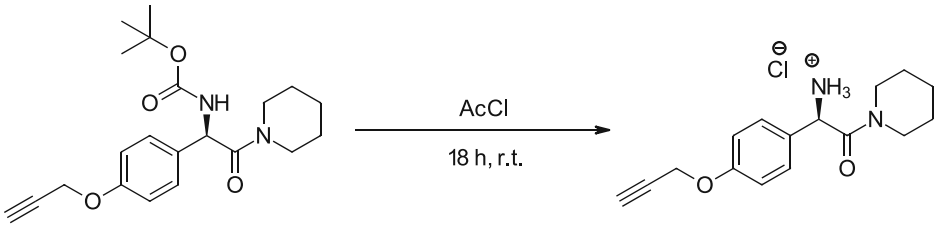

52 53

The compound was prepared according to the procedure in section 5.3.5, from (*R*)-2-oxo-2-piperidino-1-[*p*-(2-propynyloxy) phenyl ethylamino-*tert*-butylformylate (2.987 g, 0.009 mol, 1.0 eq.) and acetyl

chloride (5.447 g, 0.069 mol, 8.0 eq.) in dry methanol (22 ml), giving a brown solid (2.736 g, 99%). The product was used without further purification.

^{1}H NMR (400 MHz, $CDCl_3$) δ8.51 (s, 3H),7.42 (d, *J* = 8.7 Hz, 2H, *H*-arom), 7.07 (d, *J* = 8.7 Hz, 2H, *H*-arom), 5.47 (d, *J* = 5.3 Hz, 1H, *CH*-NH_3^+), 4.84 (d, *J* = 2.3 Hz, 2H, CH_2-O), 3.63 – 3.56 (m, 3H, CH_2-N pip + *H*C≡C), 3.22 – 3.14 (m, 2H, CH_2-N pip), 1.55 – 1.17 (m, 6H, CH_2-CH_2-CH_2 pip)

Analytical data was in accordance with literature.[97]

5.4.5 (*R*)-2-Piperidino-1-[*p*-(2-propynyloxy)phenyl]ethylamine

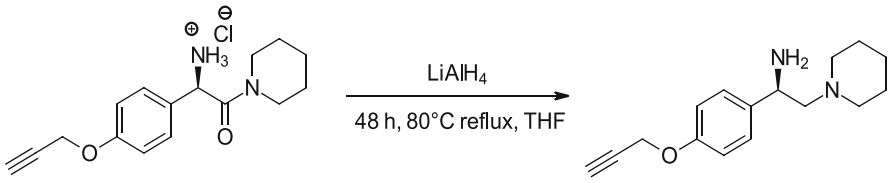

53 **54**

It was prepared according to the procedure in section 5.3.6 from (*R*)-2-oxo-2-piperidino-1-[*p*-(2-propynyloxy)phenyl]-1-ethanammonium chloride (2.678 g, 0.009 mol, 1.0 eq.) and $LiAlH_4$ (1.646 g, 0.043 mol, 5.0 eq.) in dry THF (61 ml). Column chromatography was performed for purification, giving a yellow liquid (0.299 g, 13%).

5.5 Modification of the Silica Surface

5.5.1 (3-Azidopropyl)triethoxysilane

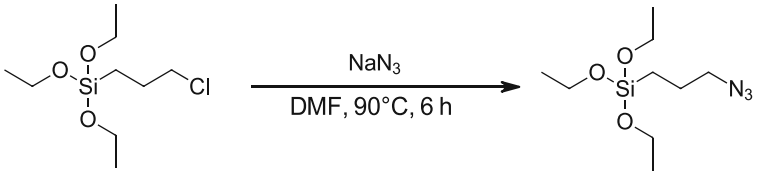

69 **46**

3-Chloropropyltriethoxysilane (5.408 g, 0.023 mol, 1.0 eq.) was dissolved in DMF (44 ml). Sodium azide (2.920 g, 0.045 mol, 2.0 eq.) was added to the solution and the mixture was heated to 90 °C and stirred for 5 h. A colourless precipitate formed, which was filtered afterwards. DMF was removed from the filtrate under vacuum (20 mbar). Again, a white precipitate formed. Et_2O was added to the suspension and was filtered over celite. Removal of the solvent gave a colourless liquid (3.710 g, 67%).

^{1}H NMR (400 MHz, $CDCl_3$) δ3.81 (q, *J* = 7.0 Hz, 6H, CH_2--O), 3.25 (t, *J* = 6.8 Hz, 2H, CH_2-Si), 1.93 – 1.83 (m, 2H, CH_2-N_3), 1.22 (t, *J* = 7.0 Hz, 9H, CH_3), 0.78 – 0.71 (m, 2H, CH_2)

Analytical data was in accordance with literature.[98]

5.5.2 Immobilization of (3-Azidopropyl)triethoxysilane on silica

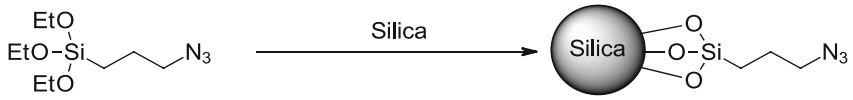

46 **47**

(3-Azidopropyl)triethoxysilane (3.710 g, 0.015 mol, 1 eq.) was dissolved in anhydrous toluene (198 ml) under argon atmosphere. Dry silica (3.710 g) was added and the mixture was sonicated for 30 minutes. The solid was isolated *via* filtration and dried under vacuum (6.920 g).

5.5.3 Click-reaction: immobilised (3-azidopropyl)triethoxysilane with (*S*)-2-Piperidino-1-[*p*-(2-propynyloxy) phenyl]ethylamine

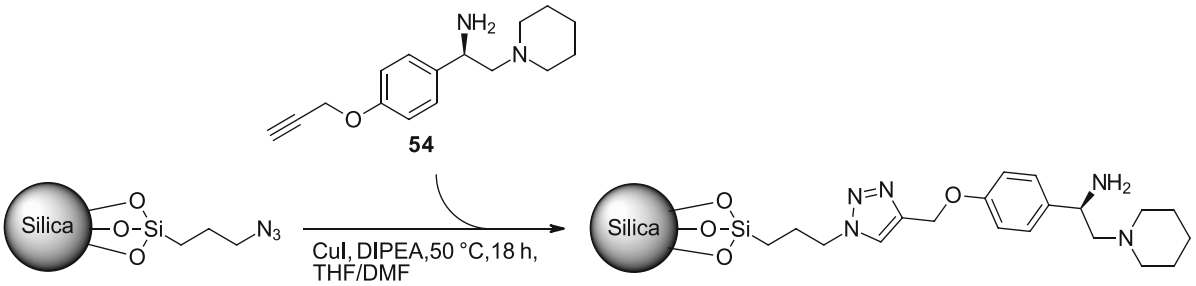

47 **48**

In a three-necked round-bottom flask (250 ml), immobilised (3-azidopropyl)triethoxysilane (1.906 g, 0.8 mmol, 1.0 eq.), *N*-ethyl-*N*-(propane-2-yl)propane-2-amine (0.299 g, 0.001 mol, 1.4 eq.), copper(I) iodide (0.031 g, 0.2 mmol, 0.2 eq.), *N*, *N*-diisopropylethylamine (1.377 g, 0.011 mol, 13.0 eq.) and a mixture of THF/DMF (1:1, 80 ml) were heated up to 50 °C and stirred for 18h, under argon atmosphere. The solid was filtered, washed ten times with methanol, seven times with acetone and dried in vacuum (20 mbar), giving a light blue solid (1.898 g).

5.6 Physisorption of the Catalyst

5.6.1 Immobilization of Catalyst with the Support of $[C_4mim]NTf_2$

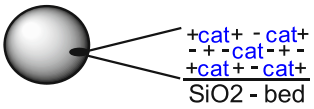

In a round-bottom flask (50ml) (*R*)-1-phenyl-2-piperidinoethylamine (0.160 g, 0.8 mmol, 1.0 eq.) and trifluoro-acetic acid (0.090 g, 0.8 mmol, 1.0 eq.) were stirred in DCM (16 ml). After 10 minutes, the solvent was removed to obtain a colourless solid. Afterwards, silica (4 g), $[C_4mim]NTf_2$ (0.800 g, 0.002 mol, 2.4 eq.) and DCM (16 ml) were added, and the mixture was stirred for 6h at room temperature. After the removal of the solvent, a colourless powder was obtained (4.495 g).

5.6.2 Immobilization of catalyst on Tungstophosphoric Acid

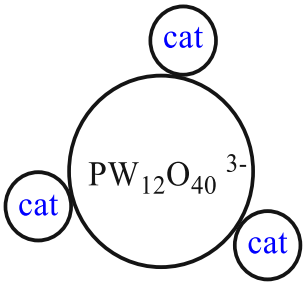

(*R*)-1-Phenyl-2-piperidinoethylamine (0.300 g, 1.5 mmol, 3.0 eq.) was dissolved in THF (6 ml). Tungstophosphoric acid (1.465 g, 0.5 mmol, 1.0 eq.) was added and the mixture was stirred for 1 h at room temperature. Volatiles were removed in vacuum (20 mbar). The obtained solid was washed several times with Et_2O and dried in vacuum (20 mbar). A greenish-grey solid remained (1.648 g).

5.7 General Screening Procedure

5.7.1 General Procedure for Parameter Optimisation of Side Chains (Diamine)

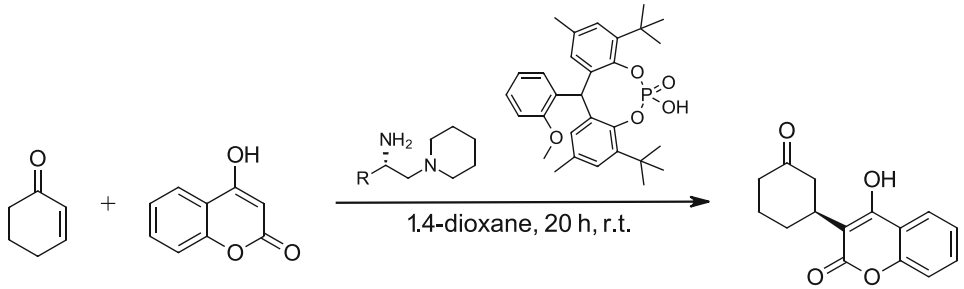

In an 8 ml vial, diamines (0.02 mmol, 0.1 eq.) and phosphoric acid (0.02 mmol, 0.1 eq.) were dissolved in 1,4-dioxane (0.7 ml, 0.3 M) and stirred for 10 minutes at room temperature. 2-Cyclohexen-1-one (1.6 mmol, 1.0 eq.) was added and the mixture was stirred for another 10 minutes, followed by addition of 4-hydroxycoumarin (1.7 mmol, 1.1 eq.). The suspension was stirred for 20 h at room

temperature. The solution was purified *via* filtration over silica in a pipette and eluted three times with Et_2O. Removal of the solvent gave a colourless solid. Conversion and enantioselectivity were determined via GC or HPLC of the crude solution.

5.7.2 General Procedure for Using $PW_{12}O_{40}^{3-}$ Immobilized Catalyst

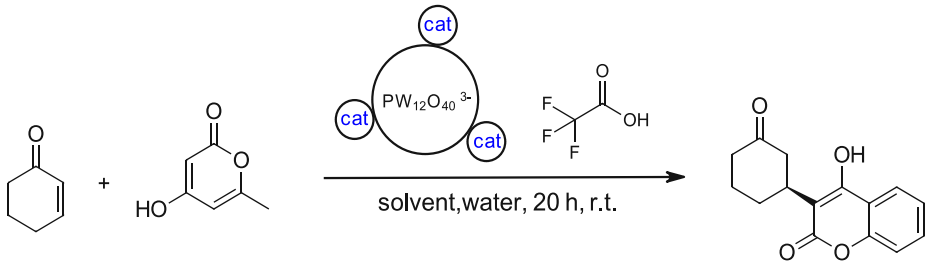

In an 8 ml vial, the immobilised diamine (0.02 mmol, 0.1 eq.) was suspended in 2-methyl-THF (0.7 ml, 0.3 M), and TFA (0.02 mmol, 0.1 eq.) was added. The suspension was stirred for 5 minutes at room temperature, followed by adding distilled water (7 µl). Afterwards, 2-cyclohexen-1-one (1.6 mmol, 1.0 eq.) was added and the mixture was stirred for another 5 minutes. Then 4-hydroxy-6-methyl-2-pyranone (1.7 mmol, 1.1 eq.) was added and the mixture was stirred for 20 h at room temperature. Purification and determination of conversion and enantioselectivity were performed identically to section 5.7.1.

5.7.3 General procedure for using a chemisorbed catalyst

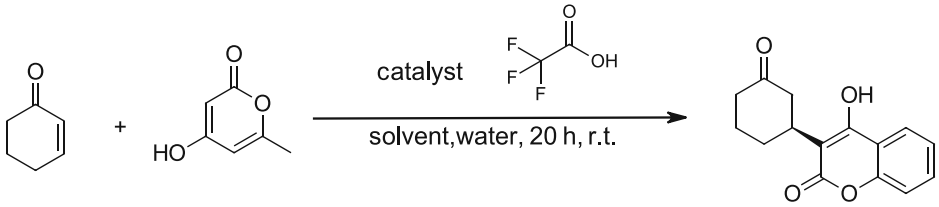

The reaction was performed precisely as in section 5.7.1, with a chemisorbed catalyst (88.23 mg). Purification and determination of conversion and enantioselectivity were performed identically to section 5.7.1.

5.7.4 General procedure for silica-physisorbed catalyst

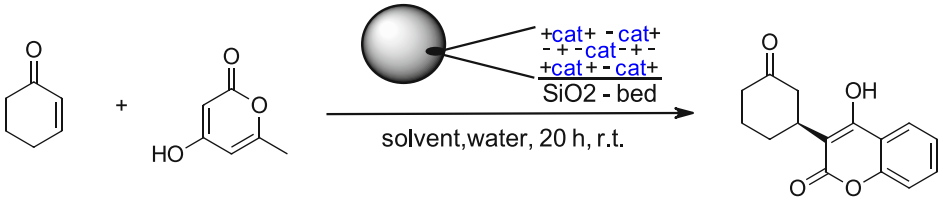

In an 8 ml vial, the immobilised diamine (0.02 mmol, 0.1 eq.) was suspended in 2-methyl-THF (0.7 ml, 0.3 M), and distilled water (7 µl) was added. Afterwards, 2-cyclohexen-1-one (1.6 mmol, 1.0 eq.) was added and the mixture was stirred for 5 minutes. Then 4-hydroxy-6-methyl-2-pyranone (1.7 mmol, 1.1

eq.) was added and the mixture was stirred for 20 h at room temperature. Purification and determination of conversion and enantioselectivity were performed identically to section 5.7.1.

5.7.5 General Procedure for Parameter Optimisation of Tertiary Amine (Diamine)

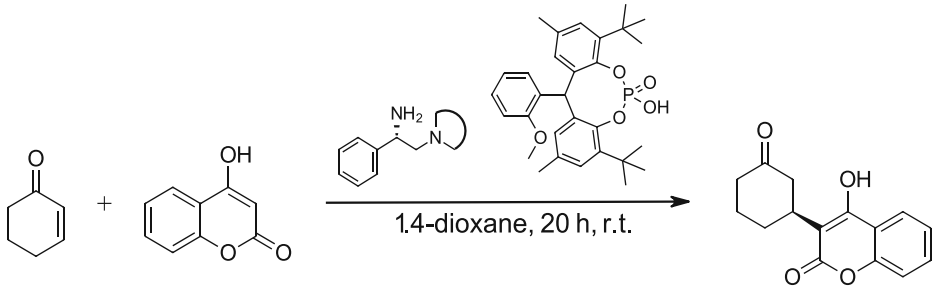

The reaction was performed precisely as in section 5.7.1 with different diamines (0.02 mmol, 0.1 eq.) and the exact component amounts. Purification and determination of conversion and enantioselectivity were performed identically to section 5.7.1.

5.7.6 General Procedure for Parameter Optimisation of Phosphoric Acids

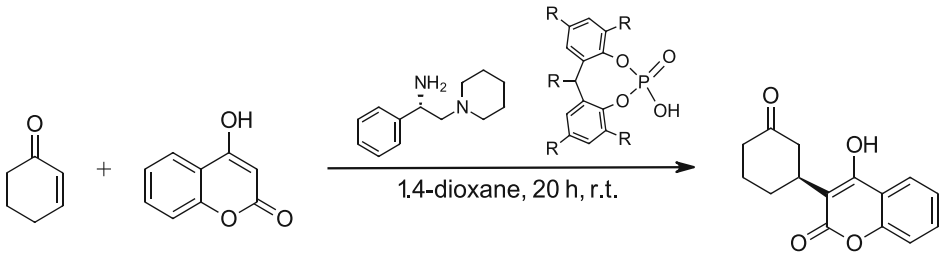

The reaction was performed precisely as in section 5.7.1 with different phosphoric acids (0.02mmol, 0.1 eq.). In an 8ml vial, diamine (0.02 mmol, 0.1 eq.) was dissolved in 1,4-dioxane (0.7 ml, 0.3 M), TFA (0.02 mmol, 0.1 eq.). The solution was stirred for 10 minutes at room temperature. Afterwards, 2-cyclohexen-1-one (1.6 mmol, 1.0 eq.) was added and the mixture was stirred for another 10 minutes. Then 4-hydroxycoumarin (1.7 mmol, 1.1 eq.) was added and the mixture was stirred for 20 h at room temperature. Purification and determination of conversion and enantioselectivity were performed identically to section 5.7.1.

5.7.7 General Procedure for Parameter Optimisation (Equivalent Screening)

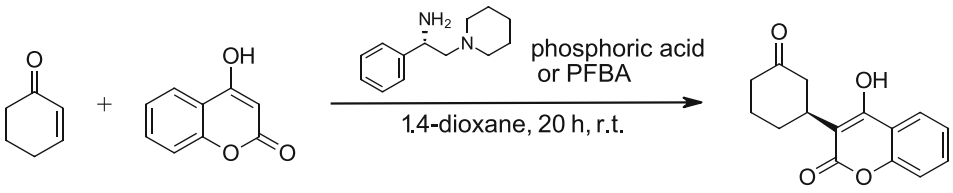

In an 8 ml vial, diamine (0.02 mmol, 0.1 eq.) and phosphoric acid (various eq.) or PFBA (0.02 mmol, 0.1 eq.) were dissolved in 1,4-dioxane (0.7 ml, 0.3 M) and stirred for 10 minutes at room temperature. 2-

Cyclohexen-1-one (1.6 mmol, 1.0 eq.) was added and the mixture was stirred for another 10 minutes, followed by 4-hydroxycoumarin (1.7 mmol, 1.1 eq.). The suspension was reacted for 20 h at room temperature. Purification and determination of conversion and enantioselectivity were performed identically to section 5.7.1.

5.7.8 General Procedure for Parameter Optimisation (Additional Water or Acid)

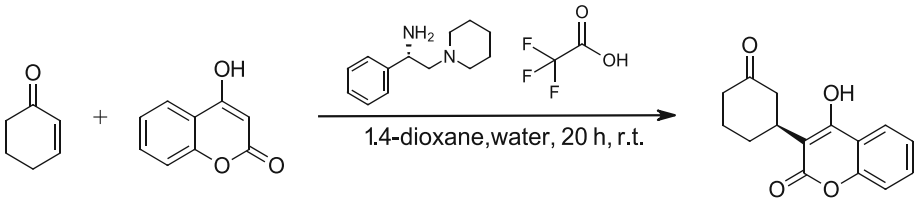

In an 8 ml vial, diamine (0.02 mmol, 0.1 eq.) was dissolved in 1,4-dioxane (0.7 ml, 0.3 M) and TFA (0.02 mmol, 0.1 eq.). The solution was stirred for 10 minutes at room temperature, followed by addition of distilled water (7 µl) or acid (7 µl). Afterwards, 2-cyclohexen-1-one (1.6 mmol, 1.0 eq.) was added and the mixture was stirred for another 10 minutes. Then 4-hydroxycoumarin (1.7 mmol, 1.1 eq.) was added, and the mixture was stirred for 20 h at room temperature. Purification and determination of conversion and enantioselectivity were performed identically to section 5.7.1.

5.7.9 General Procedure for Substrate Scope of 2-Cyclohexen-1-one- Derivatives

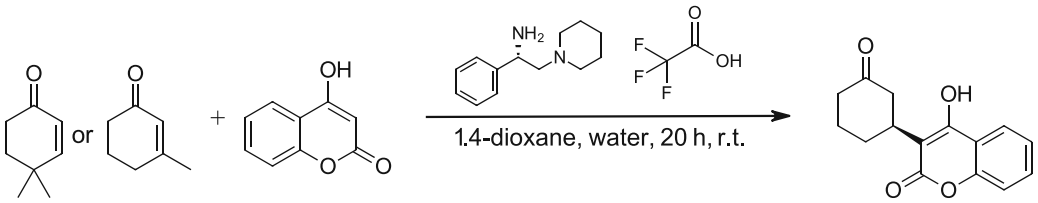

The reaction was performed precisely as in section 5.7.1, with different substrates (1.6 mmol, 1.0 eq.). Purification and determination of conversion and enantioselectivity were performed identical to section 5.7.1.

5.7.10 General Procedure for Solvent Screening

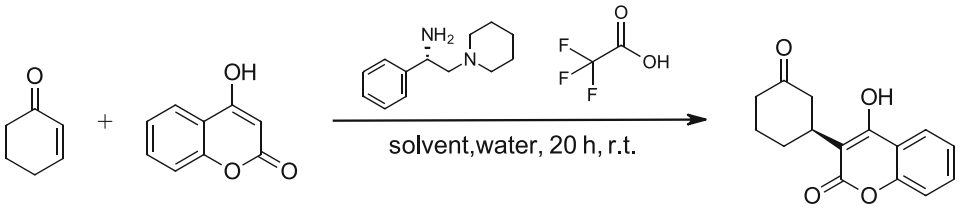

The reaction was performed precisely as in section 5.7.1, with different solvents (0.7 ml, 3.0 M). Purification and determination of conversion and enantioselectivity were performed identically to section 5.7.1.

5.7.11 General Procedure for Substrate Scope Reactants

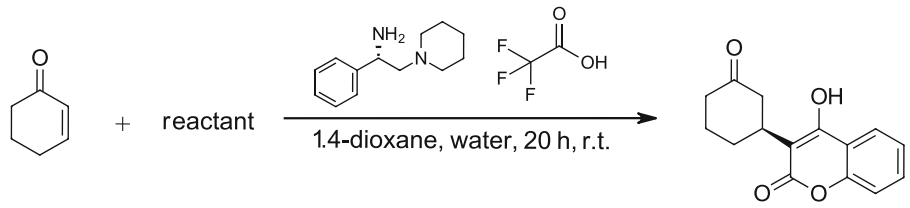

The reaction was performed precisely as in section 5.7.1, with different reactants (1.7 mmol, 1.1 eq.). Purification and determination of conversion and enantioselectivity were performed identically to section 5.7.1.

5.7.11.1 Analytical data of different products[9]

4-Hydroxycoumarin

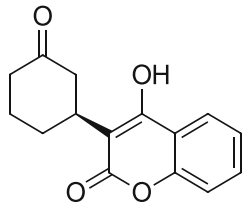

^{1}H NMR (400 MHz, $CDCl_3$)	δ 7.73 (dd, *J* = 7.9, 1.6 Hz, 1H), 7.47 – 7.41 (m, 1H), 7.25 – 7.15 (m, 2H), 3.39 (s, 1H), 3.35 (p, *J* = 3.2 Hz, 1H), 2.18 – 2.02 (m, 2H), 1.98 – 1.73 (m, 3H), 1.69 – 1.49 (m, 2H), 1.45 – 1.31 (m,1H).
^{13}C NMR (101 MHz, $CDCl_3$)	δ 160.95, 152.79, 131.59, 123.80, 122.62, 116.23, 103.04, 102.08, 38.78, 36.11, 29.39, 28.22, 19.02.
Enantiomeric excess	99% Determined *via* chiral HPLC on an ASH column (*n*-hexane/ *i*-propanol 90:10, 1 ml/min)
Yield (isolated)	89%

Analytical data was in accordance with literature.[10]

2-Hydroxy-1,4-naphthochinone

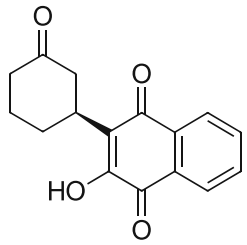

^{1}H NMR (400 MHz, $CDCl_3$)	δ 8.08 – 7.96 (m, 2H), 7.75 – 7.57 (m, 2H), 3.46 (t, *J* = 3.4 Hz, 2H), 2.45 – 1.33 (m, 9H).
^{13}C NMR (101 MHz, $CDCl_3$)	δ 210.60, 183.05, 179.26, 135.28, 133.11, 131.05, 127.11, 127.00, 126.30, 123.12, 43.86, 39.21, 34.98, 28.73, 28.34.
Enantiomeric excess	99% Determined *via* chiral HPLC on an ASH column (*n*-hexane/ *i*-propanol 90:10, 1 ml/min)
Yield (isolated)	58%

Analytical data was in accordance with literature.[10]

2-Hydroxy-6-methyl-2-pyrone

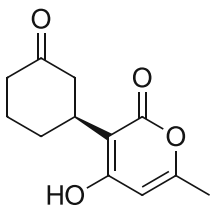

^{1}H NMR (400 MHz, $CDCl_3$)	δ 5.70(s, 1H), 3.26 (s, 1H), 3.19 (p, *J* = 3.2Hz, 2H), 2.13 (s, 3H), 2.06 – 1.91 (m, 2H), 1.82 – 1.54 (m, 4H), 1.53 – 1.25 (m, 2H).
^{13}C NMR (101 MHz, $CDCl_3$)	δ 165.87, 163.98, 160.98, 101.41, 100.32, 99.60, 38.61, 36.01, 28.66, 28.07, 19.88, 18.94.

Enantiomeric excess	99%
	Determined *via* chiral HPLC on an ASH column
	(*n*-hexane/ *i*-propanol 90:10, 1 ml/min)
Yield (isolated)	98%

Analytical data was in accordance with literature.[10]

2-Methyl-1,4-naphthochinone

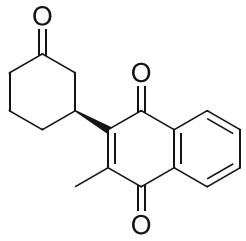

^{1}H NMR	δ 8.11 – 7.90 (m, 2H), 7.79 – 7.60 (m, 2H), 3.15 –
(400 MHz, $CDCl_3$)	2.69 (m, 4H), 3.39 (s, 1H), 3.35 (p, *J* = 3.2 Hz, 1H),
	1.71 – 1.38 (m, 6H), 0.89 – 0.67 (m, 2H).
^{13}C NMR	δ 210.64, 199.93, 195.25, 143.81, 143.10, 134.82,
(101 MHz, $CDCl_3$)	134.63, 133.50, 131.72, 127.83, 126.29, 51.42,
	41.23, 38.00, 30.55, 25.14, 22.02.
Enantiomeric excess	Not detectable
	Determined *via* chiral HPLC on an ASH column
	(*n*-hexane/ *i*-propanol 90:10, 1 ml/min)
Yield (isolated)	11%

Analytical data was in accordance with literature.[10]

Warfarin

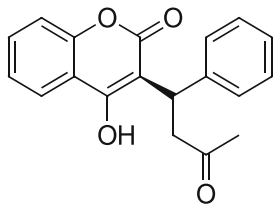

^{1}H NMR	δ 7.74 (dd, *J* = 8.0, 1.6 Hz, 1H), 7.50 – 7.30 (m,
(400 MHz, $CDCl_3$)	1H), 7.26 – 7.05 (m, 8H), 4.17 – 3.98 (m, 2H),
	2.43 – 2.33 (m, 1H), 1.56 (2, 3H).
^{13}C NMR	δ 162.25, 159.59, 152.66, 143.22, 131.53,
(101 MHz, $CDCl_3$)	129.07, 128.60, 127.03, 126.43, 123.91, 123.62,
	122.97, 122.77, 116.38, 104.05, 100.64, 42.64,
	35.31, 27.92
Enantiomeric excess	99%
	Determined *via* chiral HPLC on an ASH column
	(*n*-hexane/ *i*-propanol 90:10, 1 ml/min)
Yield (isolated)	44%

Analytical data was in accordance with literature.[10]

6 Appendix

6.1 List of Abbreviations

$[C_4mim]NTf_2$	1-butyl-3-methylimidazoliumbis(trifluoromethylsolfonyl)imide
ε	dielectric constant (permittivity)
ΔG^0	standard Gibbs-energy
C	carbon
cat	catalyst
CFC	chlorofluorocarbon
Conv.	conversion
DCC	*N, N'*-dicyclohexylcarbodiimide
DCM	dichloromethane
DHAP	dihydroxyacetonphosphate
DMF	*N, N*-dimethylformamide
ee	enantioselective excess
Eq.	equivalent
Et_2O	diethyl ether
Et_3N	triethylamine
EtOAc	ethylacetate
Fe	iron
Fe_3O_4	magnetite
FID	flame ionisation detector
G3P	glyceraldehyde 3-phosphate
GCMS	gas chromatography mass-spectrometry
H	hydrogen
H2O	water
H_2SO_4	sulfuric acid
HCl	hydrochloric acid
$HClO_4$	perchloric acid
HOMO	**h**ighest **o**ccupied **m**oleculare **o**rbital
HPLC	high performance liquid chromatography
IL	ionic liquid
$LiAlH_4$	lithium aluminium hydride
LUMO	**l**owest **u**noccupied **m**oleculare **o**rbital

MeOH	methanol
MTBE	methyl *tert*-buthylether
N	nitrogen
Na_2SO_4	sodium sulfate
NaOH	sodium hydroxide
NMR	nuclear magnetic resonance spectroscopy
NO_2	nitro
O	oxygen
Pd	palladium
PE	petrolether
PFBA	perfluorobenzoic acid
Pip	piperidine
Ph	phenyl
phen	1,10-phenanthroline
PMO	periodic mesoporous organosilica
$POCl_3$	phosphoryl chloride
SbF_6	fluoroantimonate
SiO_2	siliciumoxide
SOMO	**s**ingle **o**ccupied **m**oleculare **o**rbital
TFA	trifluoroacetic acid
THF	tetrahydrofuran
TMS	trimethylsilyl

6.2 List of Figures

[1] J. A. Johnson, L. H. Cavallari, *Trends Cardiovasc Med* **2015**, *25*, 33–41.

[2] "Warfarin Sodium Monograph for Professionals - Drugs.com," can be found under https://web.archive.org/web/20180612143838/https://www.drugs.com/monograph/warfarin-sodium.html, **n.d.**

[3] Mutschler E., Schäfer-Korting M., *Arzneimittelwirkungen*, Stuttgart: Wissenschaftliche Verlagsgesellschaft., **2013**.

[4] H. Haberfeld, *Marcumar ® 1*, **2015**.

[5] H. P. Rang, M. M. Dale, J. M. Ritter, P. Gardner, *Pharmacology*, Churchill Livingstone, **2001**.

[6] B. H. Xie, Z. Guan, Y. H. He, *Journal of Chemical Technology and Biotechnology* **2012**, *87*, 1709–1714.

[7] Y. Yuan, L. Yang, S. Liu, J. Yang, H. Zhang, J. Yan, X. Hu, *Spectrochim Acta A Mol Biomol Spectrosc* **2017**, *176*, 183–188.

[8] Z. Dong, L. Wang, X. Chen, X. Liu, L. Lin, X. Feng, *European J Org Chem* **2009**, 5192–5197.

[9] N. Halland, T. Hansen, K. A. Jørgensen, *Angewandte Chemie - International Edition* **2003**, *42*, 4955–4957.

[10] J. W. Xie, L. Yue, W. Chen, W. Du, J. Zhu, J. G. Deng, Y. C. Chen, *Org Lett* **2007**, *9*, 413–415.

[11] A. S. Kucherenko, A. A. Kostenko, G. M. Zhdankina, O. Y. Kuznetsova, S. G. Zlotin, *Green Chemistry* **2018**, *20*, 754–759.

[12] S. V. Kochetkov, A. S. Kucherenko, S. G. Zlotin, *Org Biomol Chem* **2018**, *16*, 6423–6429.

[13] K. J. Laidler, A. Cornish-Bowden, *ELIZABETH FULHAME AND THE DISCOVERY OF CATALYSIS: 100 YEARS BEFORE BUCHNER*, **1997**.

[14] C. E. Mortimer, U. Müller, *Chemie*, Georg Thieme Verlag KG, **2010**.

[15] G. Wedler, H.-J. Freund, *Physikalische Chemie*, Wiley-VCH Verlag GmbH & Co.. KGaA, **2012**.

[16] P. Atkins, D. J. Paula, *Physical Chemistry*, Oxford University Press, **2010**.

[17] Albrecht. Berkessel, Harald. Gröger, *Asymmetric Organocatalysis : From Biomimetic Concepts to Applications in Asymmetric Synthesis*, Wiley-VCH, **2005**.

[18] W. S. Knowles, S. J. Sabacky, *Chemical Communications (London)* **1968**, 1445–1446.

[19] J. A. Osborn, F. H. Jardine, J. F. Young, G. Wilkinson, *J. Chem. Soc. A,* **1966**, 1711–1732.

[20] H. Sundén, M. Engqvist, J. Casas, I. Ibrahem, A. Córdova, *Angewandte Chemie (International ed.)* **2004**, *43*, 6532–6535.

[21] A. Córdova, H. Sundén, M. Engqvist, I. Ibrahem, J. Casas, *J Am Chem Soc* **2004**, *126*, 8914–8915.

[22] S. Mukherjee, J. W. Yang, S. Hoffmann, B. List, *Chem Rev* **2007**, *107*, 5471–5569.

[23] A. Erkkilä, I. Majander, P. M. Pihko, *Chem Rev* **2007**, *107*, 5416–5470.

[24] G. Bredig, W. S. Fiske, *Biochem Z* **1912**, *46*, 7–23.

[25] H. Pracejus, *Justus Liebig Ann. Chem.* **1960**, 9–22.

[26] H. Pracejus, Helmut Mätje, *Journal für Praktische Chemie* **1964**, *24*, 195–205.

[27] Z. G. Hajos, D. R. Parrish, *J. Org. Chem.* **1974**, *39*, 1615–1621.

[28] U. Eder, G. Sauer, R. Wiechert, *Angewandte Chemie* **1971**, *83*, 492–493.

[29] B. List, A. L. Richard, F. C. Barbas, *J Am Chem Soc* **2000**, 2395–2396.

[30] B. List, *Tetrahedron* **2002**, *58*, 5573–5590.

[31] M. Fochi, L. Gramigna, A. Mazzanti, S. Duce, S. Fantini, A. Palmieri, M. Petrini, L. Bernardi, *Adv Synth Catal* **2012**, *354*, 1373–1380.

[32] J. M. Berg, J. L. Tymoczko, L. Stryer, *Stryer Biochemie*, Springer Berlin Heidelberg, Berlin, Heidelberg, **2013**.

[33] B. B. Snider, *J Am Chem Soc* **2005**, *127*, 10119–10120.

[34] *Org Process Res Dev* **2007**, *11*, 926–926.

[35] J.-L. Reymond, Y. Chen, *J. Org. Chem* **1995**, *60*, 6970–6979.

[36] F. Tanaka, C. F. Barbas, *ChemInform* **2005**, *36*, no-no.

[37] G. Wittig, H. Blumenthal, *Chem. Ber.* **1927**, *60*, 1085–1094.

[38] C. Mannich, H. Davidsen, *Chem. Ber.* **1936**, *69*, 2106–2112.

[39] G. Stork, R. Terrell, J. Szmuszkovicz, *J. Am. Chem. Soc.* **1954**, *76*, 2029.

[40] G. Stork, H. K. Lamdesman, *J. Am. Chem. Soc.* **1956**, *78*, 5128.

[41] G. Stork, A. Brizzolara, H. K. Landesman, J. Szmuszkovicz, *J. Am. Chem. Soc.* **1963**, *85*, 207.

[42] Z. Rappoport, Ed. , *The Chemistry of Enamines, Part 1*, **1994**.

[43] Boy. Cornils, *Catalysis from A to Z : A Concise Encyclopedia*, Wiley-VCH, **2007**.

[44] H. Schiff, *Justus Liebigs Ann Chem* **1864**, *131*, 118–119.

[45] R. W. Layer, *Chem. Rev.* **1963**, *63*, 489–510.

[46] B. M. Trost, I. Fleming, *Comprehensive Organic Synthesis*, Pergamon Press, **1991**.

[47] E. Knoevenagel, *Chem. Ber.* **1894**, *27*, 2345–2346.

[48] E. Pollak, *Beitr. Chem. Physiol. Pathol. ("Hofmeisters Beiträge")* **1907**, *10*, 232.

[49] E. M. P. Widmark, C. A. Jeppsson, *Skand. Arch. Physiol.* **1922**, *42*, 43.

[50] K. J. Pedersen, *J. Phys. Chem.* **1934**, *38*, 559.

[51] K. J. Pedersen, *J Am Chem Soc* **1938**, *60*, 595–601.

[52] E. H. Cordes, W. P. Jencks, *J Am Chem Soc* **1962**, *84*, 826–831.

[53] G. A. Hamilton, F. H. Westheimer, *J. Am. Chem. Soc.* **1959**, *81*, 6332.

[54] I. Fridovich, F. H. Westheimer, *J Am Chem Soc* **1962**, *84*, 3208–3209.

[55] K. A. Ahrendt, C. J. Borths, D. W. C. MacMillan, *J Am Chem Soc* **2000**, *122*, 4243–4244.

[56] H. Mayr, A. R. Ofial, E.-U. Würthwein, N. C. Aust, *J Am Chem Soc* **1997**, *119*, 12727–12733.

[57] M. Marigo, T. C. Wabnitz, D. Fielenbach, K. A. Jørgensen, *Angewandte Chemie - International Edition* **2005**, *44*, 794–797.

[58] Hayashi Y., Gotoh H., Hayashi T., Shoji M., *Angew. Chem. Int. Ed.* **2005**, *44*, 4212–4215.

[59] A. Sakakura, K. Suzuki, K. Nakano, K. Ishihara, *Org Lett* **2006**, *8*, 2229–2232.

[60] N. T. S. Phan, M. Van Der Sluys, C. W. Jones, *Adv Synth Catal* **2006**, *348*, 597–597.

[61] K. Ishihara, K. Nakano, *J Am Chem Soc* **2005**, *127*, 13079–13079.

[62] N. J. A. Martin, B. List, *J Am Chem Soc* **2006**, *128*, 13368–13369.

[63] S. Mayer, B. List, *Angewandte Chemie - International Edition* **2006**, *45*, 4193–4195.

[64] P. Y. Bruice, O. Reiser, *Org. Chem.*, Pearson Studium, München [u.a.], **2007**.

[65] E. P. Kohler, *J. Am. Chem. Soc.* **1907**, *377*, 385.

[66] N. Halland, T. Hansen, K. A. Jørgensen, *Angew. Chem. – Int. Ed.,* **2003**, *42*, 4955–4957.

[67] D. W. C. Macmillan, S. Rendler, *2 Enantioselective Organo-SOMO Catalysis: A Novel Activation Mode for Asymmetric Synthesis*, Wiley, **2012**.

[68] T. D. Beeson, A. Mastracchio, J.-B. Hong, K. Ashton, D. W. C. MacMillan, *Science (AAAS)* **2007**, *316*, 582–585.

[69] H. Kim, D. W. C. MacMillan, *J Am Chem Soc* **2008**, *130*, 398–399.

[70] H.-Y. Jang, J.-B. Hong, D. W. C. MacMillan, *J Am Chem Soc* **2007**, *129*, 7004–7005.

[71] F. Bozso, G. Ertl, M. Grunze, M. Weiss, *J Catal* **1977**, *49*, 18–41.

[72] R. Imbihl, R. J. Behm, G. Ertl, W. Moritz, *Surf Sci* **1982**, *123*, 129–140.

[73] G. Ertl, S. B. Lee, M. Weiss, *Surf Sci* **1982**, *114*, 515–526.

[74] G. Ertl, *J. Vac. Sci. & Techn. A: Vacuum, Surfaces, and Films* **1983**, *1*, 1247–1253.

[75] S. T. Bai, G. De Smet, Y. Liao, R. Sun, C. Zhou, M. Beller, B. U. W. Maes, B. F. Sels, *Chem Soc Rev* **2021**, *50*, 4259–4298.

[76] M. Benaglia, A. Puglisi, *Catalyst Immobilization: Methods and Applications*, Wiley-VCH, **2020**.

[77] D. Douroumis, I. Onyesom, M. Maniruzzaman, J. Mitchell, *Crit Rev Biotechnol* **2013**, *33*, 229–245.

[78] X. Liu, N. Zhang, D. Wang, D. Zhu, Q. Yuan, X. Zhang, L. Qian, H. Niu, Y. Lu, G. Ren, K. Tian, H. Yuan, *Cancer Sci* **2018**, *109*, 1147–1157.

[79] J. G. Croissant, X. Cattoën, M. Wong Chi Man, J.-O. Durand, N. M. Khashab, *Nanoscale* **2015**, *7*, 2318–2334.

[80] Y.-H. Lee, X.-Q. Zhang, W. Zhang, M.-T. Chang, C.-T. Lin, K.-D. Chang, Y.-C. Yu, J. T.-W. Wang, C.-S. Chang, L.-J. Li, T.-W. Lin, *Advanced materials (Weinheim)* **2012**, *24*, 2320–2325.

[81] M. Fujiwara, K. Shiokawa, Y. Tanaka, Y. Nakahara, *Chemistry of materials* **2004**, *16*, 5420–5426.

[82] Y. Chen, N. Liu, Y. et al. Cao, *Sci. Rep.* **2016**, *6*, 32540.

[83] T. Yokoi, T. Karouji, S. Ohta, J. N. Kondo, T. Tatsumi, *Chemistry of materials* **2010**, *22*, 3900–3908.

[84] N. Haraguchi, N. Takenaka, A. Najwa, Y. Takahara, M. K. Mun, S. Itsuno, *Adv. Synth. Catal.* **2018**, *360*, 112–113.

[85] M. Hatano, T. Miyamoto, K. Ishihara, *Org. Lett.* **2007**, *9*, 4535–4538.

[86] G. L. Khatik, V. Kumar, V. A. Nair, *Org. Lett.* **2012**, *14*, 2442–2445.

[87] S. H. van Leeuwen, P. J. L. M. Quaedflieg, Q. B. Broxterman, R. M. J. Liskamp, *Tetrahedron Lett* **2002**, *43*, 9203–9207.

[88] K. Wechakorn, P. Chanpanich, P. Kamkalong, S. Anantachisilp, *Orient J Chem* **2019**, *35*, 1054–1061.

[89] P. Riente, J. Yadav, M. A. Pericàs, *Org Lett* **2012**, *14*, 3668–3671.

[90] H. Hagiwara, T. Kuroda, T. Hoshi, T. Suzuki, *Adv Synth Catal* **2010**, *352*, 909–916.

[91] S. Luo, J. Li, H. Xu, L. Zhang, J.-P. Cheng, *Org Lett* **2007**, *9*, 3675–3678.

[92] M. A. Schmidt, E. A. Reiff, X. Qian, C. Hang, V. C. Truc, K. J. Natalie, C. Wang, J. Albrecht, A. G. Lee, E. T. Lo, Z. Guo, A. Goswami, S. Goldberg, J. Pesti, L. T. Rossano, *Org Process Res Dev* **2015**, *19*, 1317–1322.

[93] S. H. Van Leeuwen, P. J. L. M. Quaedflieg, Q. B. Broxterman, R. M. J. Liskamp, *Tetrahedron Let*, **2002**, 43, 9203-9207

[94] G. L. Khatik, V. Kumar, V. A. Nair, *Org Lett* **2012**, *14*, 2442–2445.

[95] M. Felber, M. Bauwens, J. M. Mateos, S. Imstepf, F. M. Mottaghy, R. Alberto, *Chemistry - A European Journal* **2015**, *21*, 6090–6099.

[96] N. Haraguchi, N. Takenaka, A. Najwa, Y. Takahara, M. K. Mun, S. Itsuno, *Adv Synth Catal* **2018**, *360*, 112–123.

[97] M. Hatano, T. Miyamoto, K. Ishihara, *Org Lett* **2007**, *9*, 4535–4538.

[98] K. Wechakorn, P. Chanpanich, P. Kamkalong, S. Anantachisilp, *Oriental Journal of Chemistry* **2019**, *35*, 1054–1061.